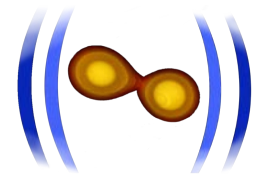




PennState
Eberly College of Science



Explosive Astrophysics: Binary Neutron Star Mergers

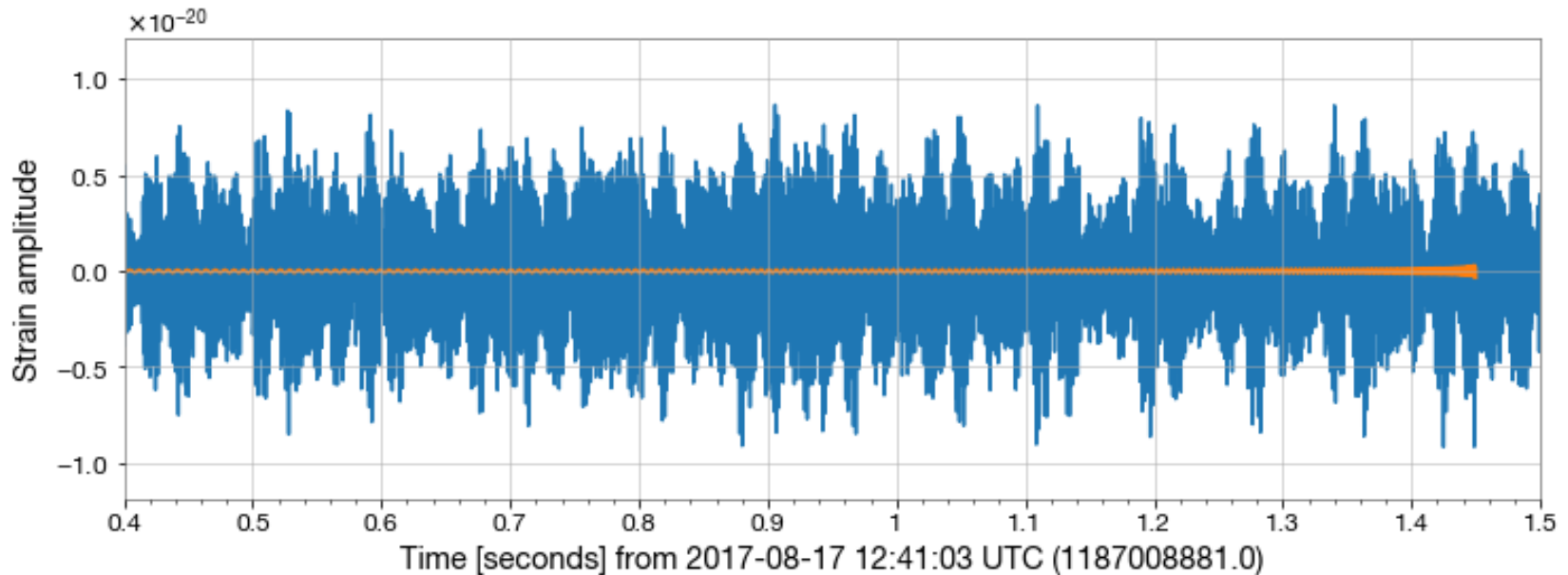
David Radice (Penn State)





Learning objectives

- Key ideas in numerical relativity
- The physics in neutron-star black-hole and double neutron-star mergers



- Gravitational wave astronomy needs accurate theoretical predictions to interpret observations
- Understand the dynamics of core-collapse supernovae, mergers, gamma-ray bursts, ...
- Enable multi-messenger astrophysics

$$R_{\mu\nu} - \frac{1}{2} g_{\mu\nu} R = 8\pi T_{\mu\nu}$$

*Spacetime tells matter how to move
matter tells spacetime how to curve.*

– John Archibald Wheeler

$$R_{\mu\nu} - \frac{1}{2} g_{\mu\nu} R = 8\pi T_{\mu\nu}$$

*Spacetime tells matter how to move
matter tells spacetime how to curve.*

– John Archibald Wheeler

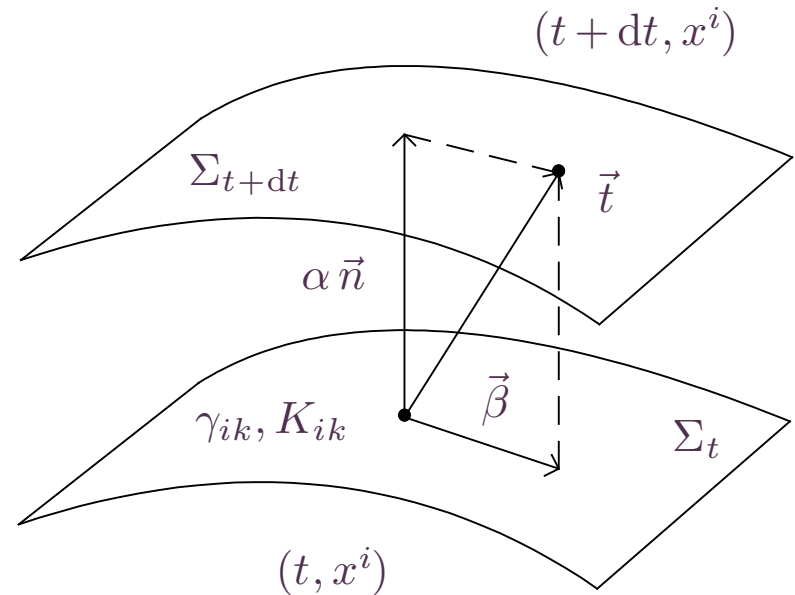
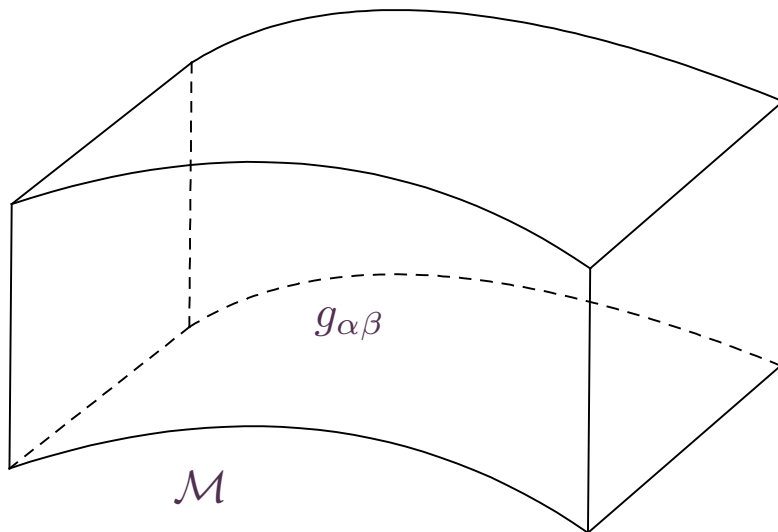
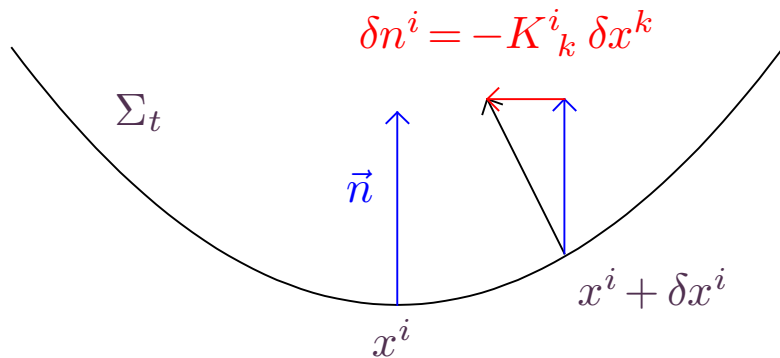


Figure. From spacetime to back to space and time.

The three metric defines distances on the 3-hypersurface: $ds^2 = \gamma_{ik} dx^i dx^k$.



The external curvature is defined as

$$K_{\mu\nu} = -\gamma^\alpha_\mu \gamma^\beta_\nu \nabla_\alpha n_\beta.$$

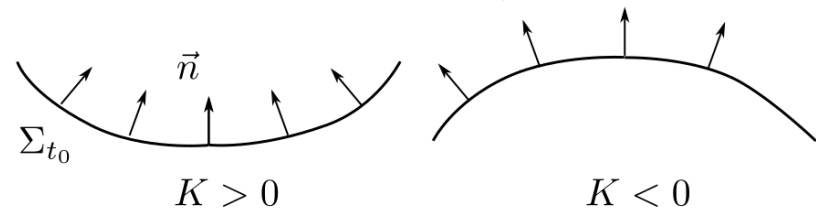
The external curvature measures the rate of change of \vec{n} across Σ_t .

The extrinsic curvature can also be defined in terms of the Lie derivative of γ_{ik} :

$$K_{ik} = -\frac{1}{2} \mathcal{L}_{\vec{n}} \gamma_{ik} = -\frac{1}{2\alpha} (\partial_t + \mathcal{L}_{\vec{\beta}}) \gamma_{ik}.$$

The trace of the extrinsic curvature measures the expansion of the worldlines of the normal observers:

$$K = -\nabla_\mu n^\mu.$$



The ADM equations are obtained by taking projections of Einstein's field equations:

Hamiltonian constraint

$$R + K^2 - K_{ik} K^{ik} = 16 \pi \rho$$

Momentum constraint

$$D_k K^k_i - D_i K = 8 \pi S_i$$

Evolution of γ_{ik}

$$\partial_t \gamma_{ik} - \mathcal{L}_{\vec{\beta}} \gamma_{ik} = -2 \alpha K_{ik}$$

Evolution of K_{ik}

$$\begin{aligned} \partial_t K_{ik} - \mathcal{L}_{\vec{\beta}} K_{ik} = & 8 \pi \left(S_{ik} - \frac{1}{2} \gamma_{ik} (S - \rho) \right) \\ & - D_i D_k \alpha + \alpha (R_{ik} - 2 K_{ij} K^j_k + K K_{ik}) \end{aligned}$$

- Two constraint equations. Analogous to Gauss' law in E&M theory.
- Two evolution equations. Analogous to Faraday's and Ampere's laws in E&M.
- The ADM equations are weakly hyperbolic (unstable).

How many degrees of freedom are there in the theory?

$$\underbrace{12}_{\gamma_{ik}, K_{ik}} - \underbrace{4}_{\text{gauge}} - \underbrace{4}_{\text{constraints}} = \underbrace{4}_{h_{+, \times}, \dot{h}_{+, \times}}$$

Ideally, we would like to prescribe (γ_{ik}, K_{ik}) at $t=0$ as the initial data. However, γ_{ik} and K_{ik} need to satisfy the constraints...

- We need to specify only a portion of the initial data and compute the rest using the Hamiltonian and momentum constraint.
- It is not obvious how to choose: an unwise choice would lead to a mathematical problem without solutions.

Two standard approaches:

1. Conformal decomposition (Bowen-York initial data).
2. Conformal thin sandwich formalism

In Bowen-York initial data we set:

$$\gamma_{ik} = \psi^4 \bar{\gamma}_{ik} = \psi^4 \delta_{ik}, \quad K_{ik} = \psi^{-2} \left[2 \bar{D}^{(i} W^{k)} - \frac{2}{3} \bar{\gamma}^{ik} \bar{D}_j W^j \right].$$

The Hamiltonian and momentum equations are then solved for ψ and W^i .

- The resulting set of equations (Lichnerowicz equations) is well posed.
- The equation for W^i can be solved analytically:

$$W^i = -\frac{1}{4r} \left(7 \bar{P}^i + \frac{\bar{P}_j x^j x^i}{r^2} \right) - \frac{1}{r^3} \bar{\varepsilon}^{ij}{}_{k} \bar{J}_j x^k,$$

where $\bar{\varepsilon}_{ijk} = [ijk]$, and \bar{P}^i and \bar{J}^i are freely specified constant vectors.

- A Schwarzschild black hole has

$$\psi = 1 + \frac{m}{2r}, \quad W^i = 0.$$

- Most common application: puncture initial data.

Consider the Schwarzschild metric

$$ds^2 = -\left(1 - \frac{2m}{R}\right) dt^2 + \left(1 - \frac{2m}{R}\right)^{-1} dR + R^2 d\Omega^2.$$

The coordinate transformation $R = r \left(1 + \frac{m}{2r}\right)^2$ changes the line element to

$$ds^2 = -\left(\frac{1 - \frac{m}{2r}}{1 + \frac{m}{2r}}\right)^2 dt^2 + \left(1 + \frac{m}{2r}\right)^4 [dr^2 + r^2 d\Omega^2].$$

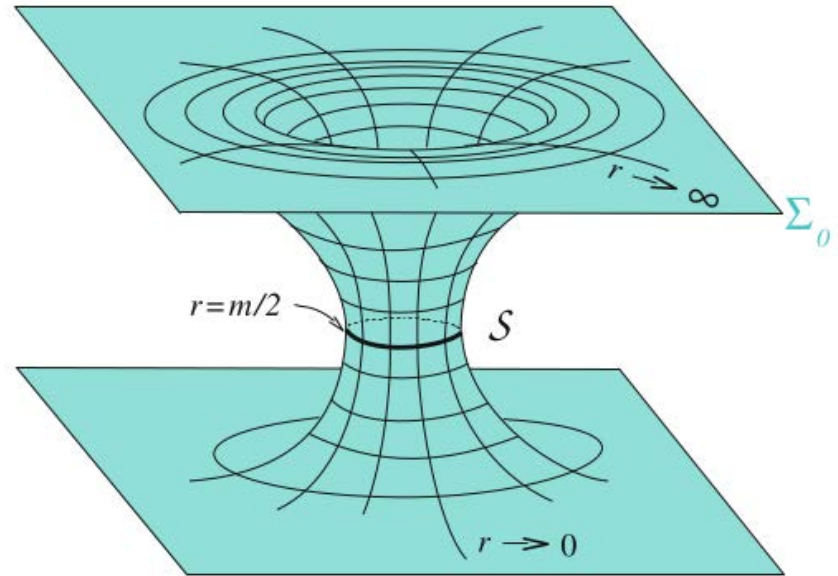
The **spatial part** of the metric is conformally flat:

$$\gamma_{ik} = \psi^4 f_{ik}, \quad \psi = 1 + \frac{m}{2r}.$$

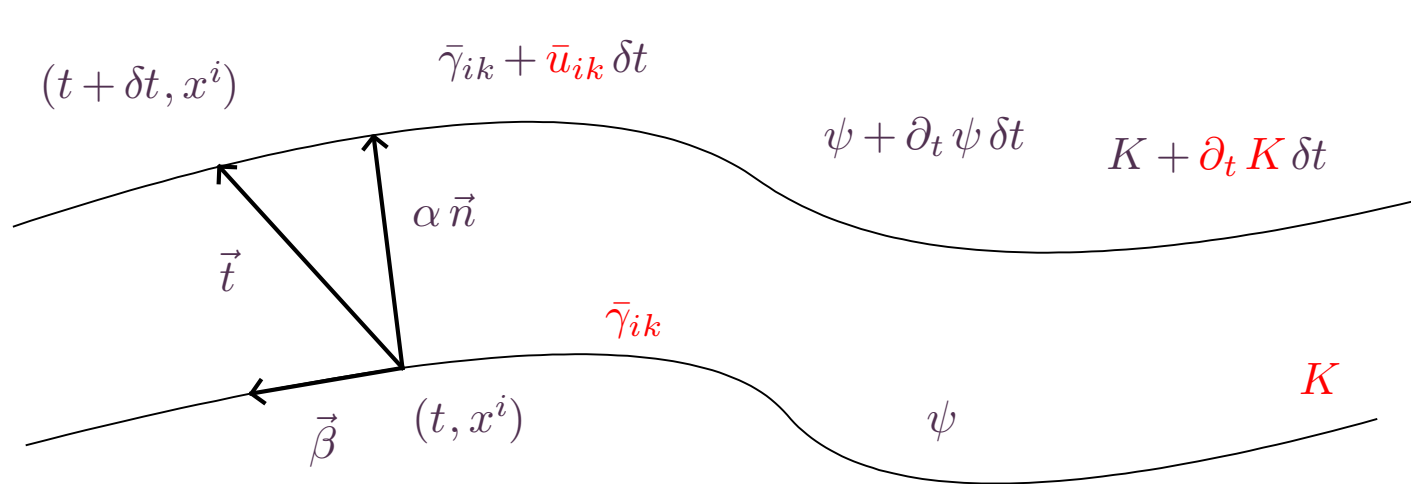
We make the coordinate transformation $r \mapsto \hat{r} = \frac{m^2}{4r}$. This leaves the point $R = 2m$, $r = \hat{r} = m/2$ and

$$dl^2 = \left(1 + \frac{m}{2\hat{r}}\right)^4 [d\hat{r}^2 + \hat{r}^2 d\Omega^2].$$

So at $r \rightarrow 0$ the spacetime is actually *flat*. Note, however that the term $\frac{1 - \frac{m}{2r}}{1 + \frac{m}{2r}}$ changes sign at $r = m/2$.



From Gourgouhlon, *3+1 Formalism in General Relativity*, Lecture Notes in Physics 846 (2012).



The conformal thin sandwich combines constraint and evolution equations.

The most commonly used XCTS formalism has free data

$$\bar{\gamma}_{ik}, \quad \bar{u}_{ik} := \partial_t \bar{\gamma}_{ik}, \quad K, \quad \partial_t K.$$

This approach is very general and used for NS-NS and BH-NS initial data, but more complex to implement, not so well understood mathematically.

The Z4 formalism extends Einstein equations as (Gundlach et al. 2005)

$$R_{\mu\nu} - \frac{1}{2} g_{\mu\nu} R + \nabla_{\mu} Z_{\nu} + \nabla_{\nu} Z_{\mu} - \kappa_1 [t_{\mu} Z_{\nu} + t_{\nu} Z_{\mu} - (1 + \kappa_2) g_{\mu\nu} t^{\mu} Z^{\nu}] = 8 \pi T_{\mu\nu}.$$

This systems recovers the Einstein equations when $Z_{\mu} = 0$.

With the definition $\Theta = -Z^{\mu} n_{\mu}$, the 3+1 form of the Z4 system reads

$$\begin{aligned} (\partial_t - \mathcal{L}_{\vec{\beta}}) \gamma_{ik} &= -2 \alpha K_{ik}, \\ (\partial_t - \mathcal{L}_{\vec{\beta}}) K_{ik} &= 8 \pi \left(S_{ik} - \frac{1}{2} \gamma_{ik} (S - \rho) \right) - D_i D_k \alpha + \alpha [R_{ik} + D_i Z_j + D_j Z_i - 2 K_{ij} K^j_k \\ &\quad + (K - 2\Theta) K_{ik} - \kappa_1 (1 + \kappa_2) \gamma_{ik} \Theta], \\ (\partial_t - \mathcal{L}_{\vec{\beta}}) \Theta &= \frac{\alpha}{2} \left[R + (K - 2\Theta) K - K_{ik} K^{ik} - 16 \pi \rho + 2 D_j Z^j \right. \\ &\quad \left. - 2 \frac{\partial_j \alpha}{\alpha} Z^j - 2 (2 + \kappa_2) \kappa_1 \Theta \right], \\ (\partial_t - \mathcal{L}_{\vec{\beta}}) Z_i &= \alpha \left[D_k K^k_i - D_i K - 8 \pi S_i + \partial_i \Theta - \frac{\partial_i \alpha}{\alpha} \Theta - 2 K_i^k Z_k - \kappa_2 Z_i \right]. \end{aligned}$$

Constraints become evolution equations. Strongly hyperbolic. GH is a special case of Z4.

Introduced by Bernuzzi and Hilditch (2010).

- It is a conformal decomposition of Z4 that drops non principal terms.
- The resulting set of equations is very similar to BSSN, but strongly hyperbolic.
- Use puncture gauge to handle singularities without excision.

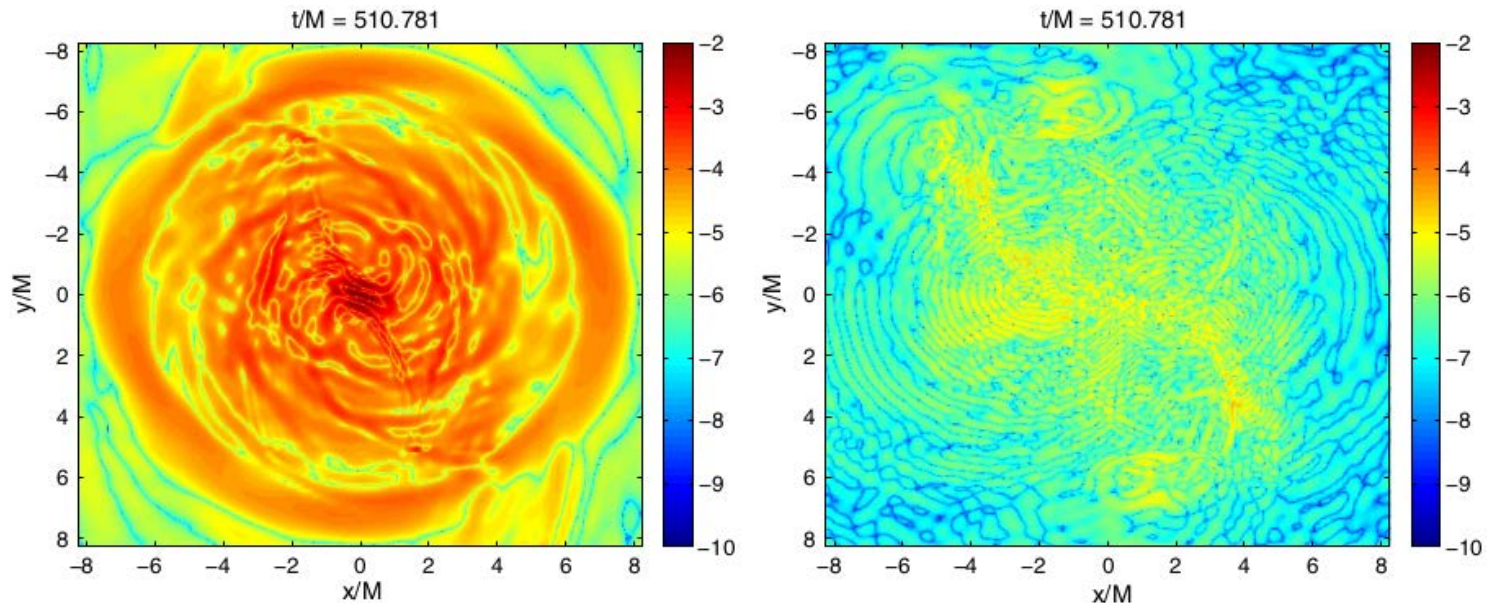
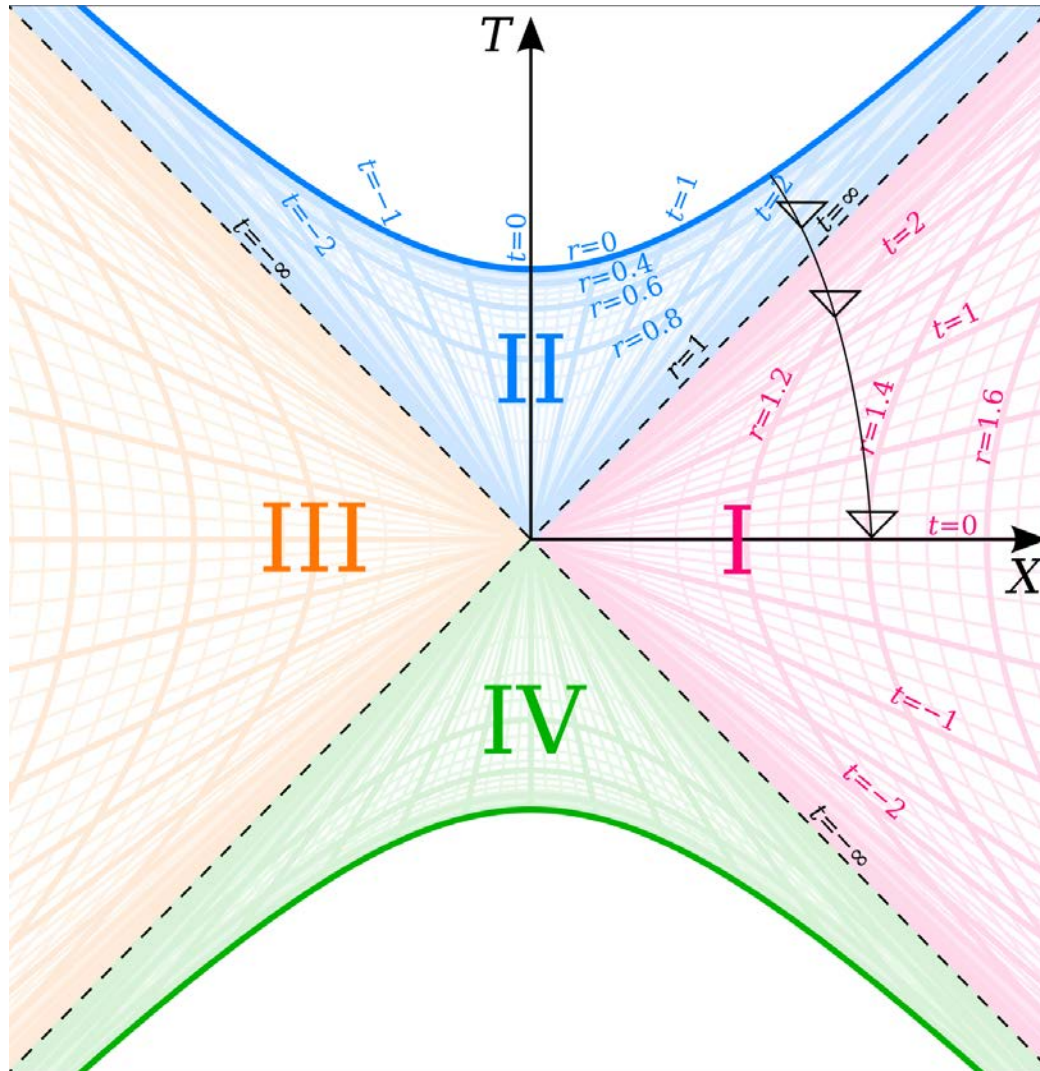


Figure. Hamiltonian constraint violation for BSSN (right) and Z4c (left) in a binary neutron star merger simulation. Hilditch, et al. (2013).



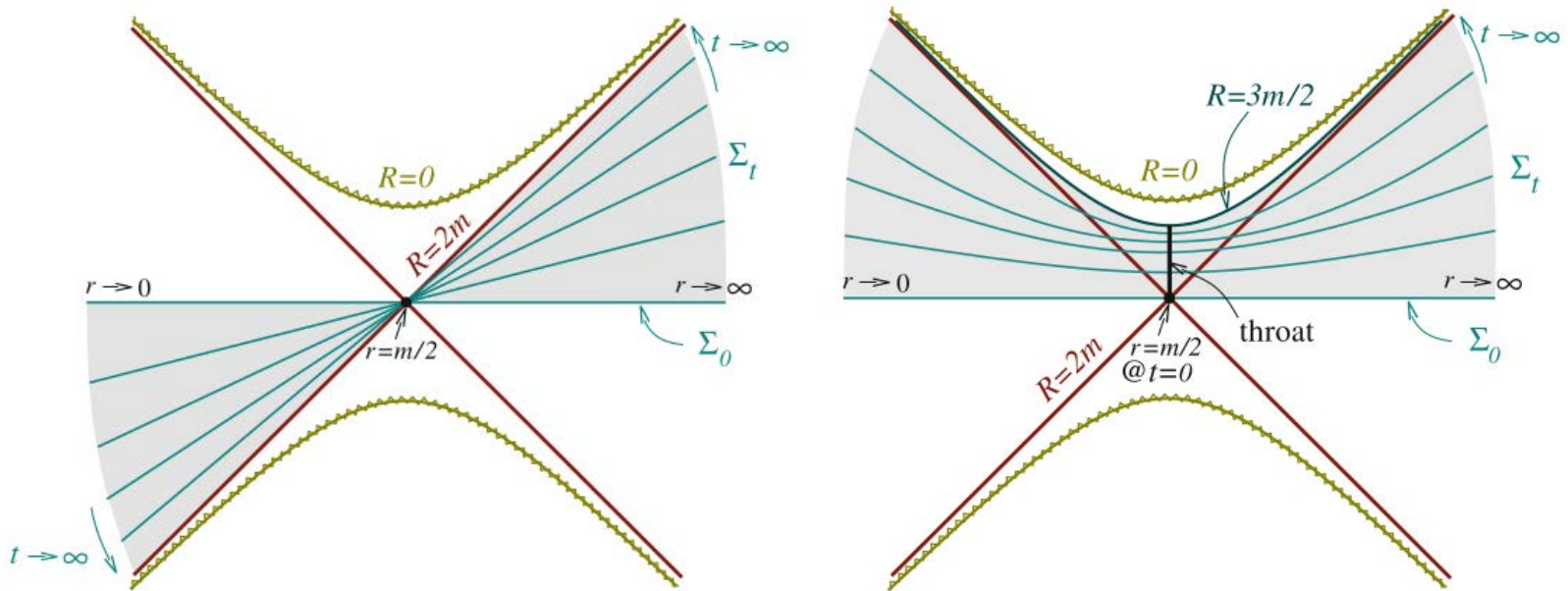


Figure. Schwarzschild slicing (left), Reinhart/Estabrook slicing (right). Fromourgouhlon 2012.

Puncture codes use variants of the moving puncture gauge (Bona+ 1995; Alcubierre+ 2003):

$$\partial_t \alpha - \beta^j \partial_j \alpha = -2 \alpha K.$$

The generalized harmonic gauge condition is an alternative way of fixing the gauge condition and transforming the Einstein equations into a set of evolution equations and constraints that does not make use of the ADM equations.

The generalized harmonic gauge condition is an alternative way of fixing the gauge condition and transforming the Einstein equations into a set of evolution equations and constraints that does not make use of the ADM equations.

The coordinates are assumed to satisfy an inhomogeneous wave equation:

$$\nabla_{\alpha} \nabla^{\alpha} x^{\mu} = H^{\mu},$$

where H^{μ} is a prescribed function of the coordinates ($H^{\mu} = 0$ leads to the harmonic gauge). The LHS of the equation can be written as

$$\nabla_{\alpha} \nabla^{\alpha} x^{\mu} = \frac{1}{|g|^{1/2}} \partial_{\nu} (|g|^{1/2} g^{\mu\nu}) = -\Gamma^{\mu} = -g^{\alpha\beta} \Gamma^{\mu}_{\alpha\beta},$$

where $\Gamma^{\alpha}_{\beta\gamma}$ are the four-dimensional Christoffel symbols.

The generalized harmonic gauge condition is an alternative way of fixing the gauge condition and transforming the Einstein equations into a set of evolution equations and constraints that does not make use of the ADM equations.

The coordinates are assumed to satisfy an inhomogeneous wave equation:

$$\nabla_{\alpha} \nabla^{\alpha} x^{\mu} = H^{\mu},$$

where H^{μ} is a prescribed function of the coordinates ($H^{\mu} = 0$ leads to the harmonic gauge). The LHS of the equation can be written as

$$\nabla_{\alpha} \nabla^{\alpha} x^{\mu} = \frac{1}{|g|^{1/2}} \partial_{\nu} (|g|^{1/2} g^{\mu\nu}) = -\Gamma^{\mu} = -g^{\alpha\beta} \Gamma^{\mu}_{\alpha\beta},$$

where $\Gamma^{\alpha}_{\beta\gamma}$ are the four-dimensional Christoffel symbols.

The GHG then reads

$$\Gamma^{\mu} = -H^{\mu}.$$

The generalized harmonic formulation is obtained by replacing derivatives in the Ricci tensor with Γ^μ and then setting $\Gamma^\mu = -H^\mu$:

$$R_{\alpha\beta} = -\frac{1}{2} g^{\mu\nu} \partial_\mu \partial_\nu g_{\alpha\beta} - \nabla_{(\alpha} H_{\beta)} + g^{\gamma\delta} g^{\varepsilon\varphi} (\partial_\varepsilon g_{\gamma\alpha} \partial_\varphi g_{\delta\beta} - \Gamma_{\alpha\gamma\varepsilon} \Gamma_{\beta\delta\varphi}),$$

where $\Gamma_{\alpha\beta\gamma} = g_{\alpha\mu} \Gamma^\mu_{\beta\gamma}$.

In vacuum Einstein equations are simply $R_{\alpha\beta} = 0$. In the GHG, these equations take the form of a nonlinear wave equation:

$$g^{\mu\nu} \partial_\mu \partial_\nu g_{\alpha\beta} = -2 \nabla_{(\alpha} H_{\beta)} + 2 g^{\gamma\delta} g^{\varepsilon\varphi} (\partial_\varepsilon g_{\gamma\alpha} \partial_\varphi g_{\delta\beta} - \Gamma_{\alpha\gamma\varepsilon} \Gamma_{\beta\delta\varphi}).$$

With constraints now given by

$$\mathcal{C}^\mu = \Gamma^\mu + H^\mu = 0.$$

The first-order reduction of this system of equations is implemented in SpEC (SXS collaboration).

Consider a small perturbation around flat background: $\gamma_{ik} = \delta_{ik} + h_{ik}$. Einstein equations say

$$\partial_t^2 h_{ik} = \nabla^2 h_{ik} - \partial_i \Gamma_k - \partial_k \Gamma_i.$$

Consider a small perturbation around flat background: $\gamma_{ik} = \delta_{ik} + h_{ik}$. Einstein equations say

$$\partial_t^2 h_{ik} = \nabla^2 h_{ik} - \partial_i \Gamma_k - \partial_k \Gamma_i.$$

The Γ_i 's are defined as

$$\Gamma_i = \partial_m h^m_i - \frac{1}{2} \partial_i h.$$

Consider a small perturbation around flat background: $\gamma_{ik} = \delta_{ik} + h_{ik}$. Einstein equations say

$$\partial_t^2 h_{ik} = \nabla^2 h_{ik} - \partial_i \Gamma_k - \partial_k \Gamma_i.$$

The Γ_i 's are defined as

$$\Gamma_i = \partial_m h^m_i - \frac{1}{2} \partial_i h.$$

Note that in the TT gauge $\Gamma_i \equiv 0$. Harmonic coordinates are a generalization of the TT gauge!

Matter is evolved using the conservation laws of energy and momentum:

$$\nabla_\nu T^{\mu\nu} = 0,$$

where

$$T_{\mu\nu} = T_{\mu\nu}^{(\text{hd})} + T_{\mu\nu}^{(\text{rad})} + T_{\mu\nu}^{(\text{em})}.$$

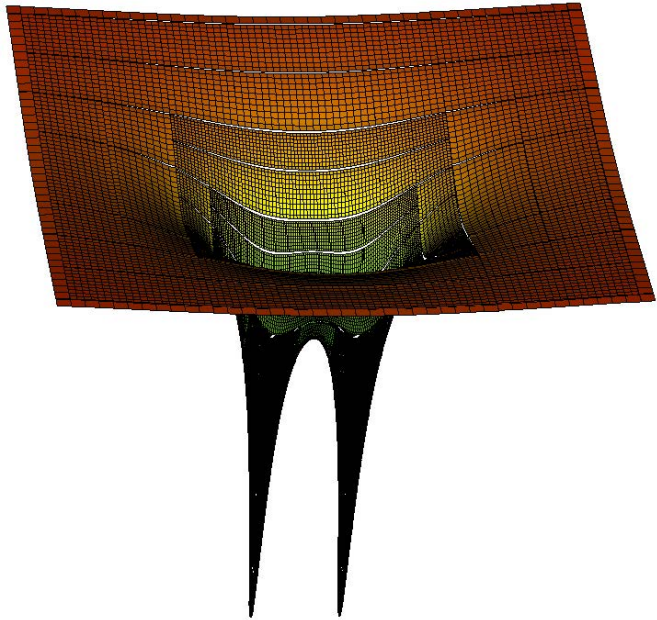
These equations are closed using

- Constitutive relations, such as the equation of state $p = p(\rho, T, \{Y_i\})$ and the Ohm's law.
- Conservation, balance laws for the different particle species:

$$\frac{dY_A}{ds} = u^\mu \nabla_\mu Y_A = \sum_B (R_{B \rightarrow A} - R_{A \rightarrow B}).$$

- The Boltzmann equations for the conservation of the neutrino number in phase space

$$p^\alpha \left[\frac{\partial F}{\partial x^\alpha} - \Gamma^\beta_{\alpha\gamma} p^\gamma \frac{\partial F}{\partial p^\beta} \right] = \mathbb{C}[F].$$



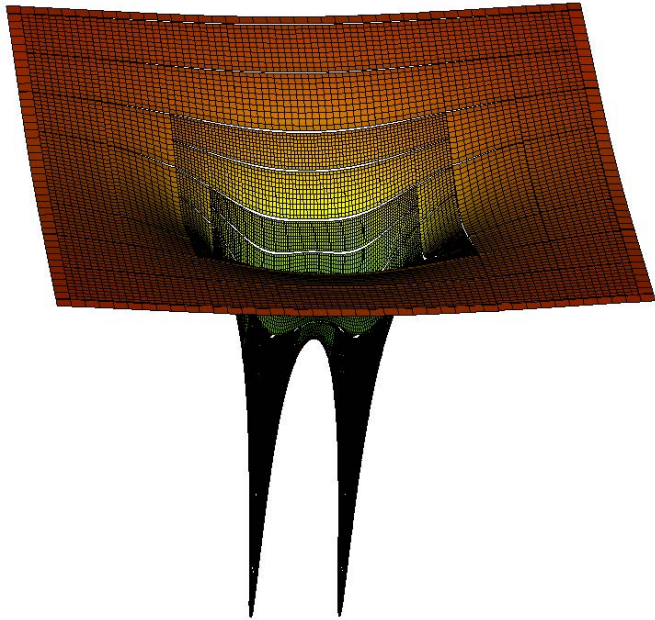
The approach followed in all numerical relativity codes is to discretize first in space then in time (method of lines).

Example.

$$\partial_t u + \partial_x u = 0 \implies \frac{du_i}{dt} = -\frac{u_{i+1} - u_{i-1}}{2 \Delta x}.$$

Derivatives can be discretized using finite-differences, spectral, or Galerkin methods.

So-called high-resolution shock capturing schemes (HRSC) are needed to handle shocks in the (M)HD equations.



The approach followed in all numerical relativity codes is to discretize first in space then in time (method of lines).

Example.

$$\partial_t u + \partial_x u = 0 \implies \frac{du_i}{dt} = -\frac{u_{i+1} - u_{i-1}}{2 \Delta x}.$$

Derivatives can be discretized using finite-differences, spectral, or Galerkin methods.

So-called high-resolution shock capturing schemes (HRSC) are needed to handle shocks in the (M)HD equations.

Exercise. Choose a recent numerical relativity paper.

- Which formulations were used to create the initial data and to evolve the Einstein's equations?
- Which numerical methods and codes were used? Are they publicly available?
- Which steps would be necessary to reproduce the work?

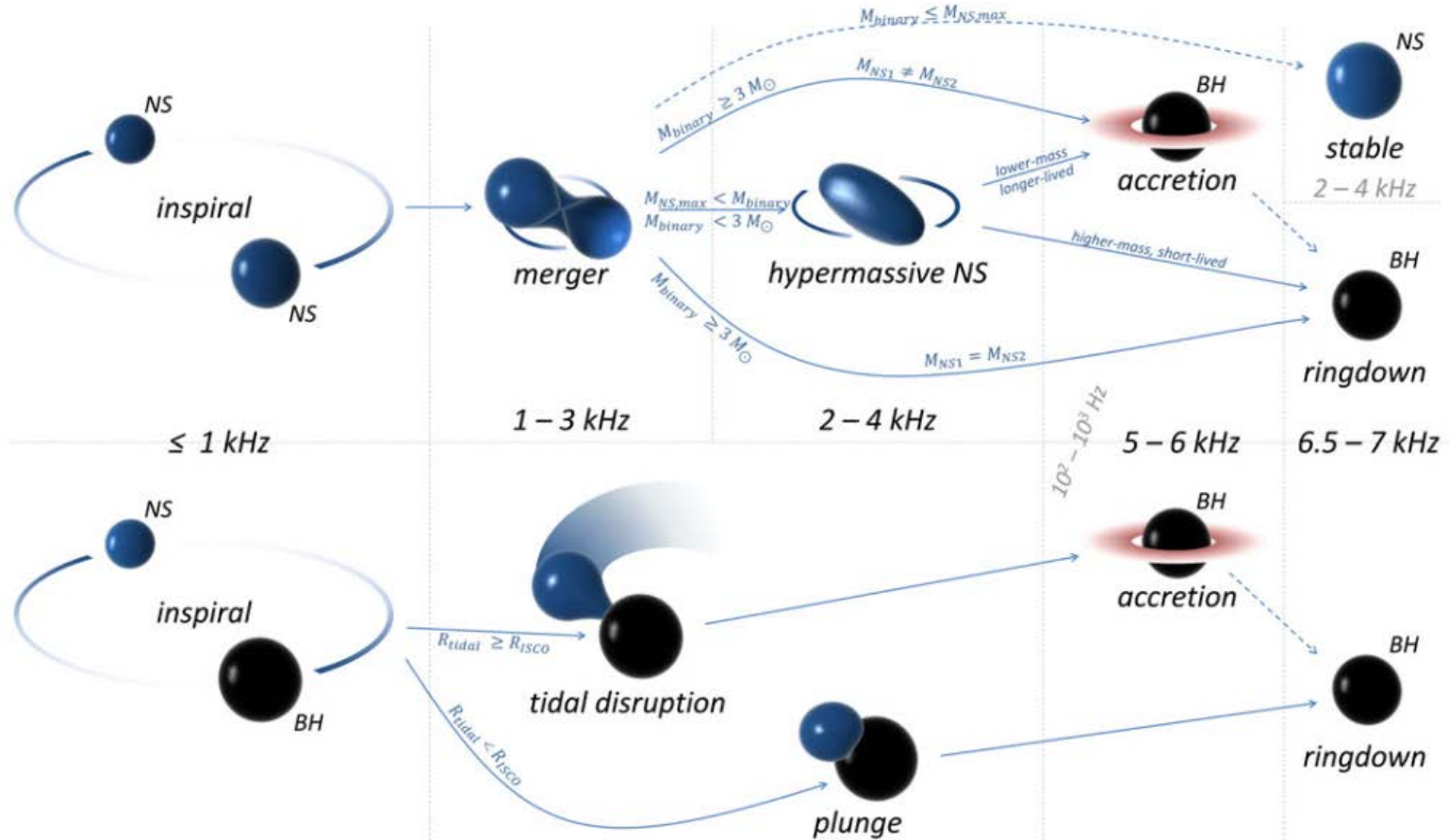


Figure. From Bartos, Brady, and Márka (2013).

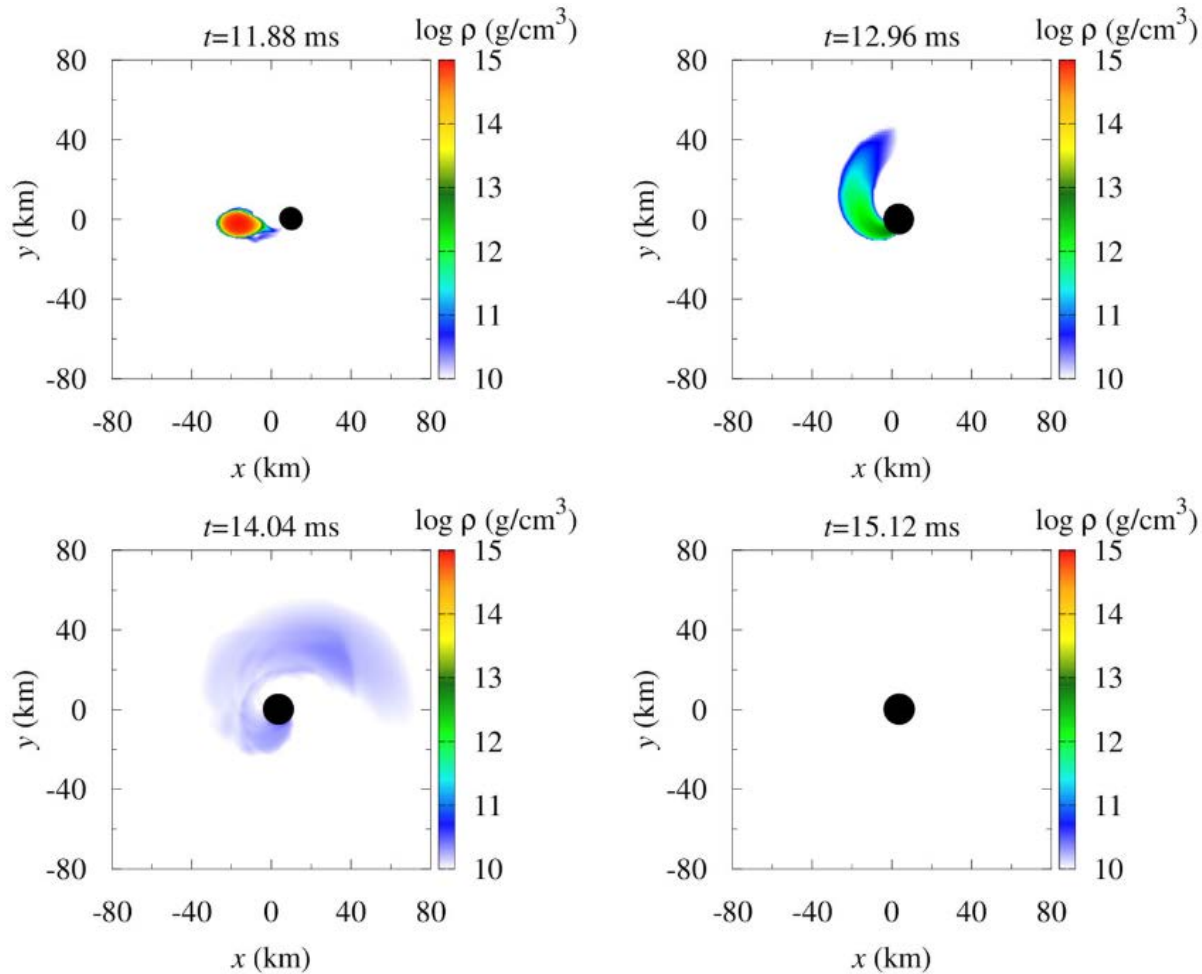


Figure. EM dark BHNS merger, from Kyutoku et al. (2021).

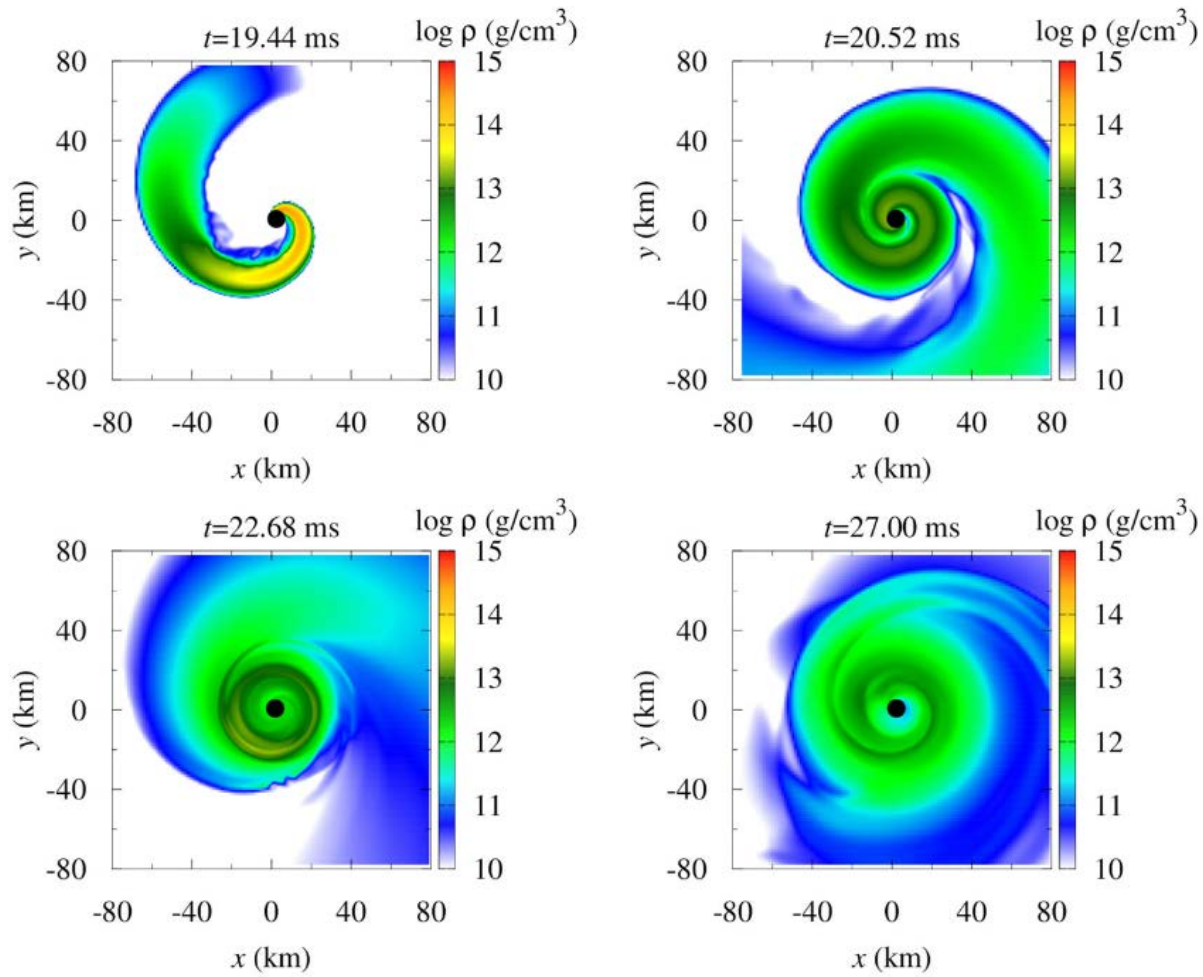
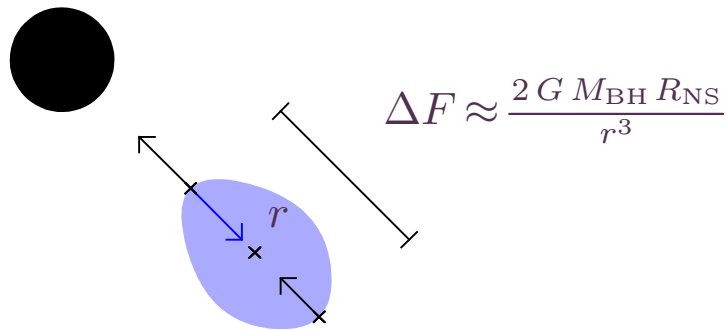


Figure. EM bright BHNS merger, from Kyutoku et al. (2021).



$$\Delta F \approx \frac{2 G M_{\text{BH}} R_{\text{NS}}}{r^3}$$

Mass shedding occurs when tidal forces exceed the self-gravity of the star:

$$r_{\text{ms}} = 2^{1/3} c_R \left(\frac{M_{\text{BH}}}{M_{\text{NS}}} \right)^{1/3} R_{\text{NS}}.$$

$$\Delta F > F_{\text{self}} \iff \frac{2 G M_{\text{BH}} R_{\text{NS}}}{r^3} > \frac{G M_{\text{NS}}}{R_{\text{NS}}^2}$$

BHNS are EM bright only if

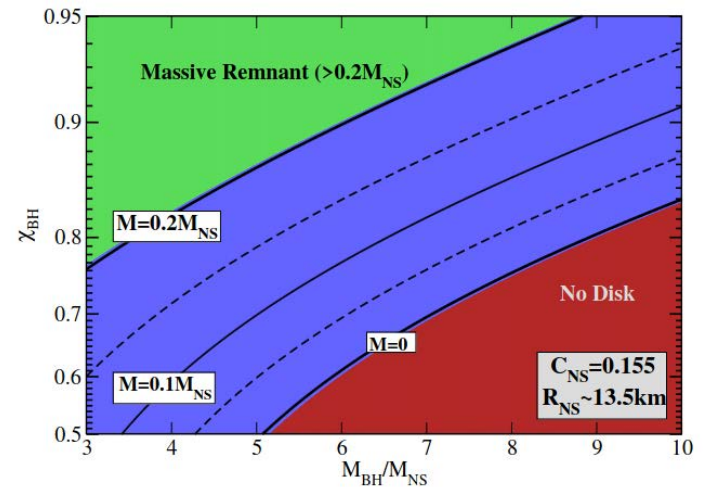
$$r_{\text{ms}} > r_{\text{ISCO}}.$$

Figure. Predicted disk mass in BHNS mergers from Foucart 2012.

Fitting formulas have been constructed for ejecta and disk mass from BHNS using r_{ISCO} , M_{BH} , R_{NS} , M_{NS} .

Similar fits also exist for NSNS mergers, but they are much less accurate.

See Krüger and Foucart (2020), Nedora et al. (2022).



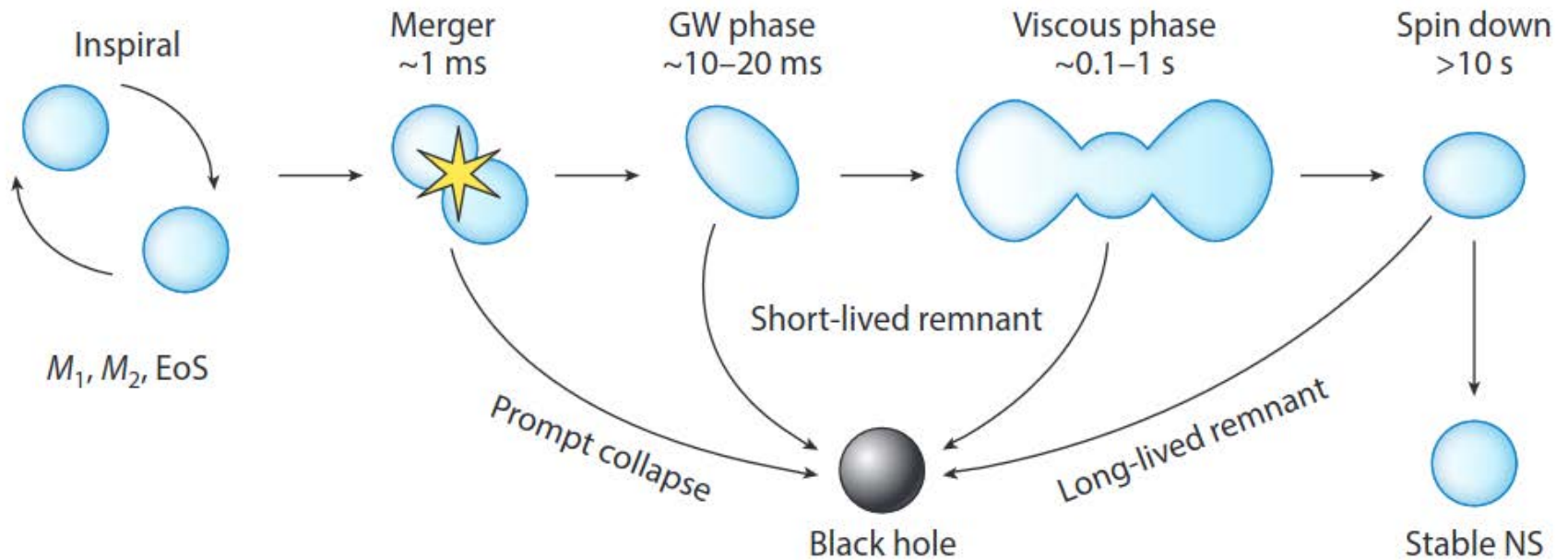
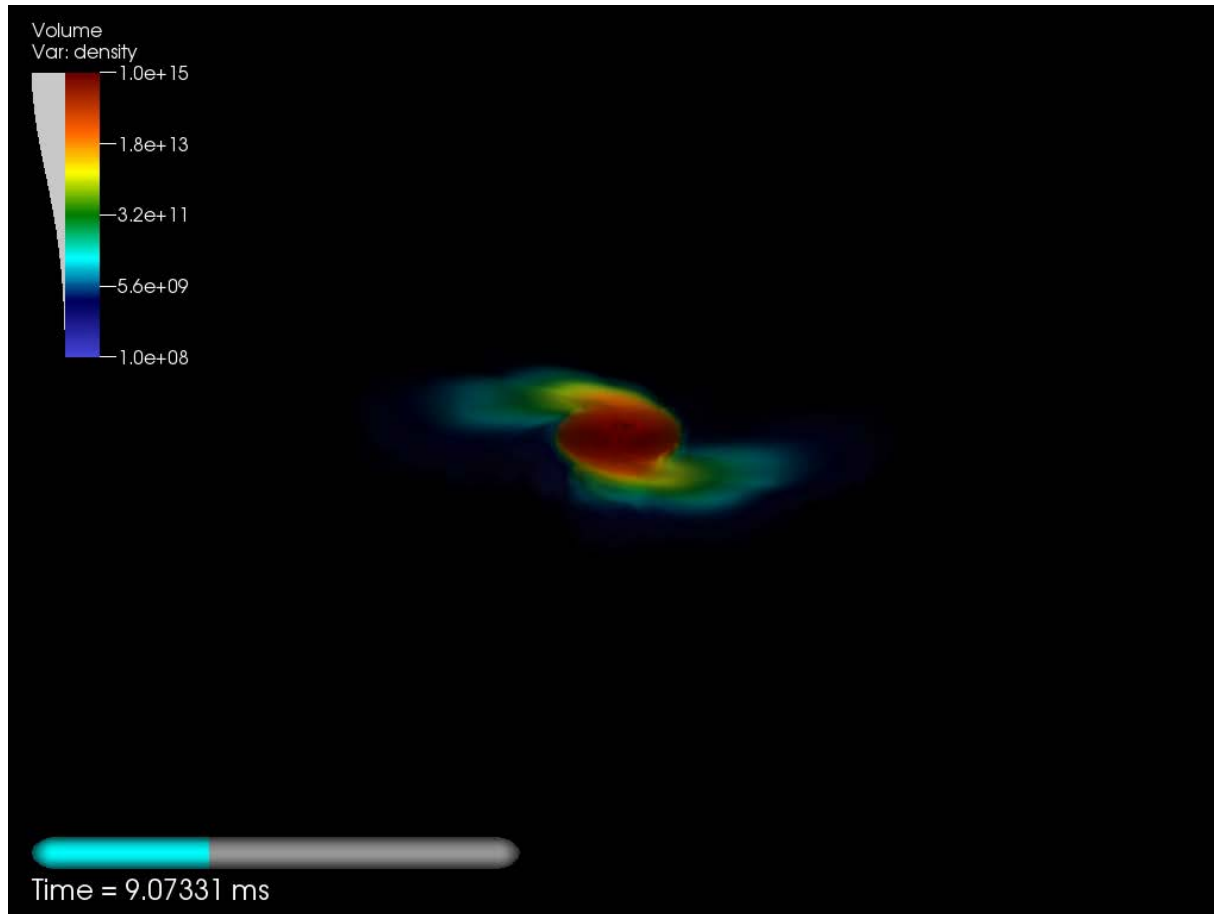


Figure. From Radice, Bernuzzi, & Perego (2020)



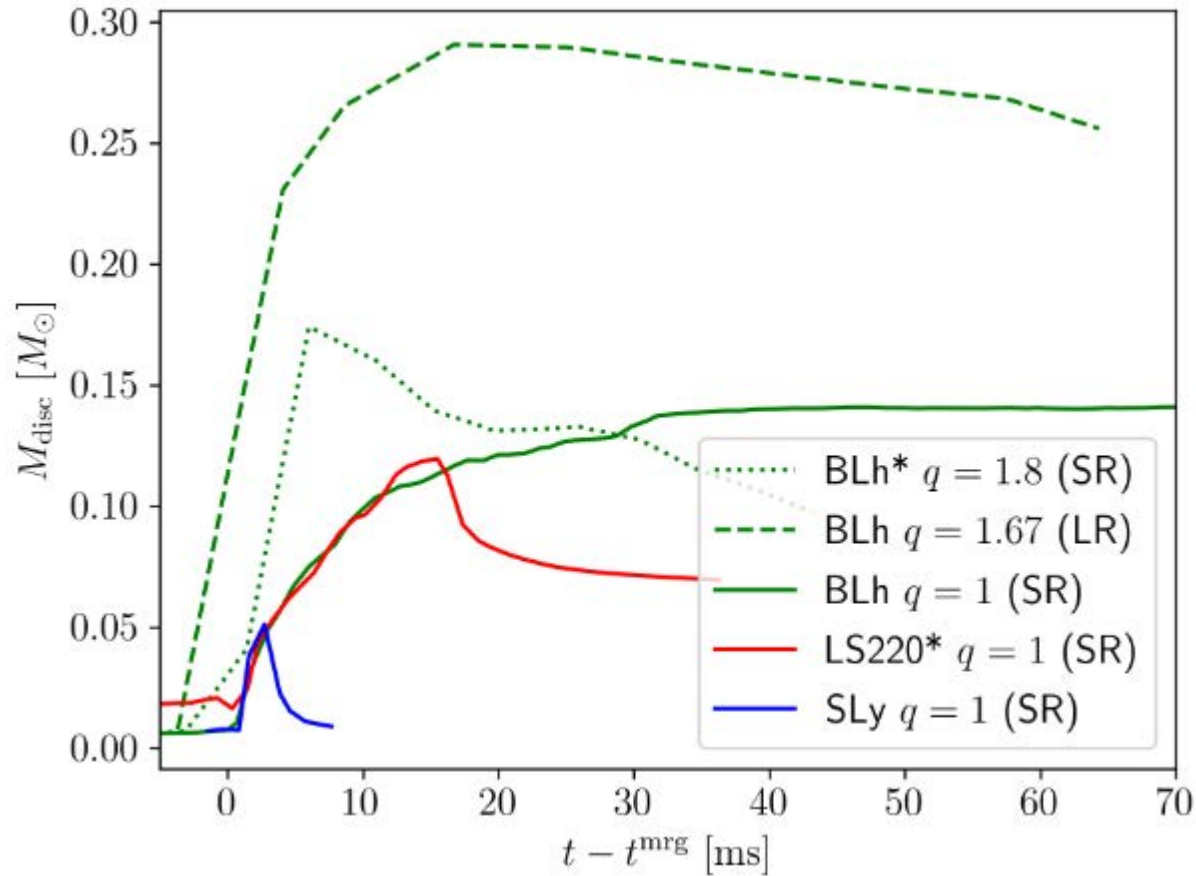
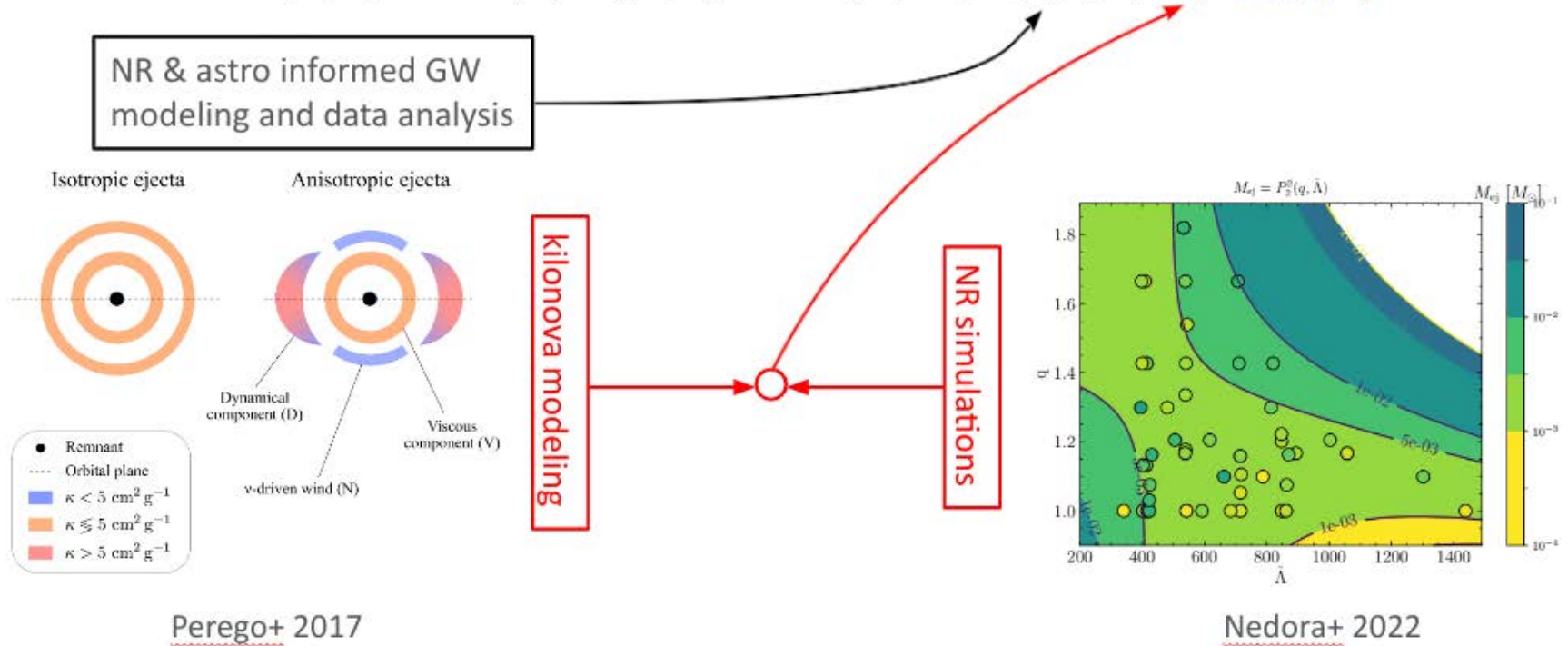


Figure. From Bernuzzi et al. (2020)

$$P[\theta|d] \sim P[\theta]P[d|\theta] = P[\theta]P[d_{\text{GW}}|\theta]P[d_{\text{EM}}|\theta]$$



- Different pipelines exist employing different fits, but all based on the same simulations.
- Excluding cases with large q , the ejecta is dominated by *late-time winds*.

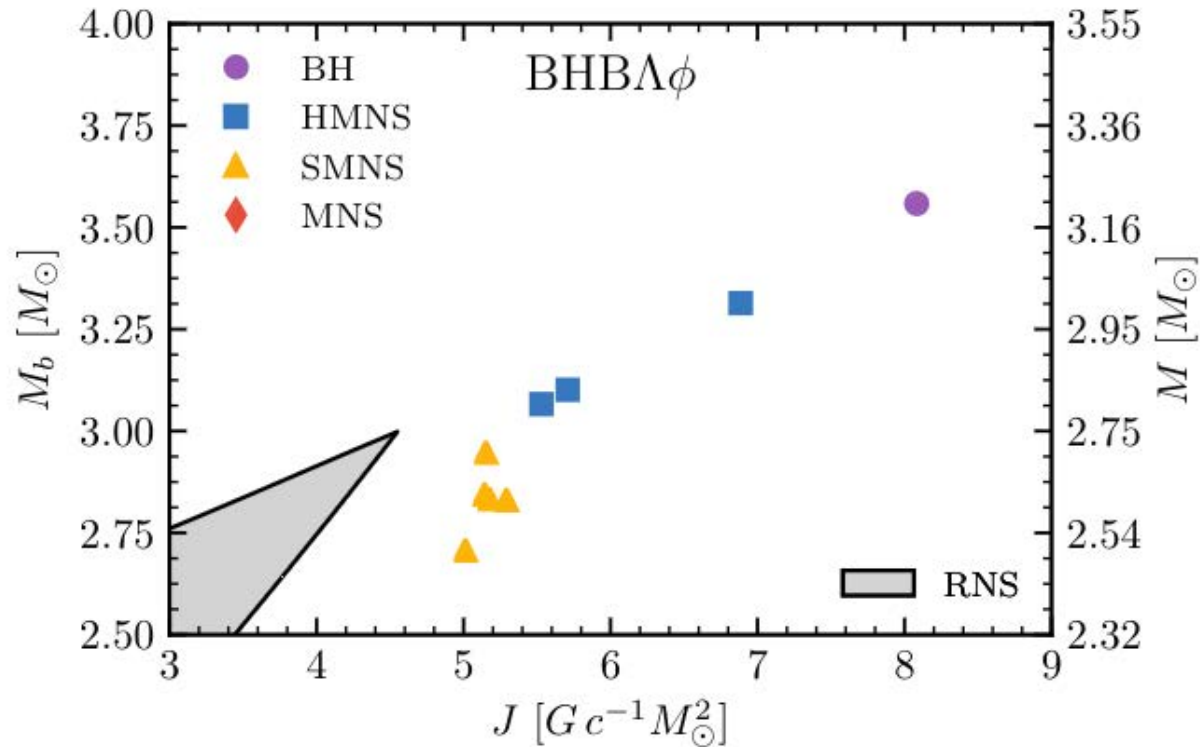


Figure. Remnants at the end of the GW dominated phase of the evolution. From Radice et al. (2018).

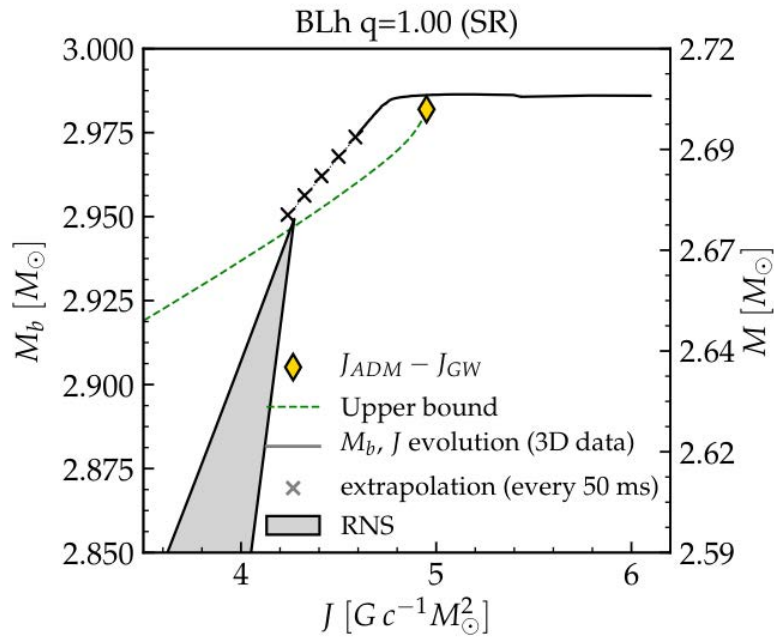


Figure. From Nedora et al. (2020)

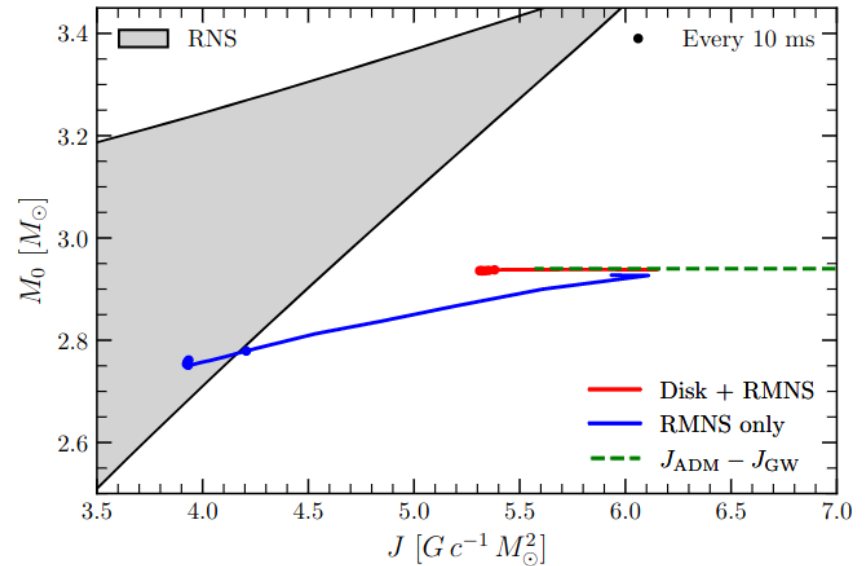


Figure. From Radice & Bernuzzi (2023)

- Evolution of massive NS merger remnants is not well understood
- Outcome of mergers depends on complex interplay of MHD turbulence and neutrino physics

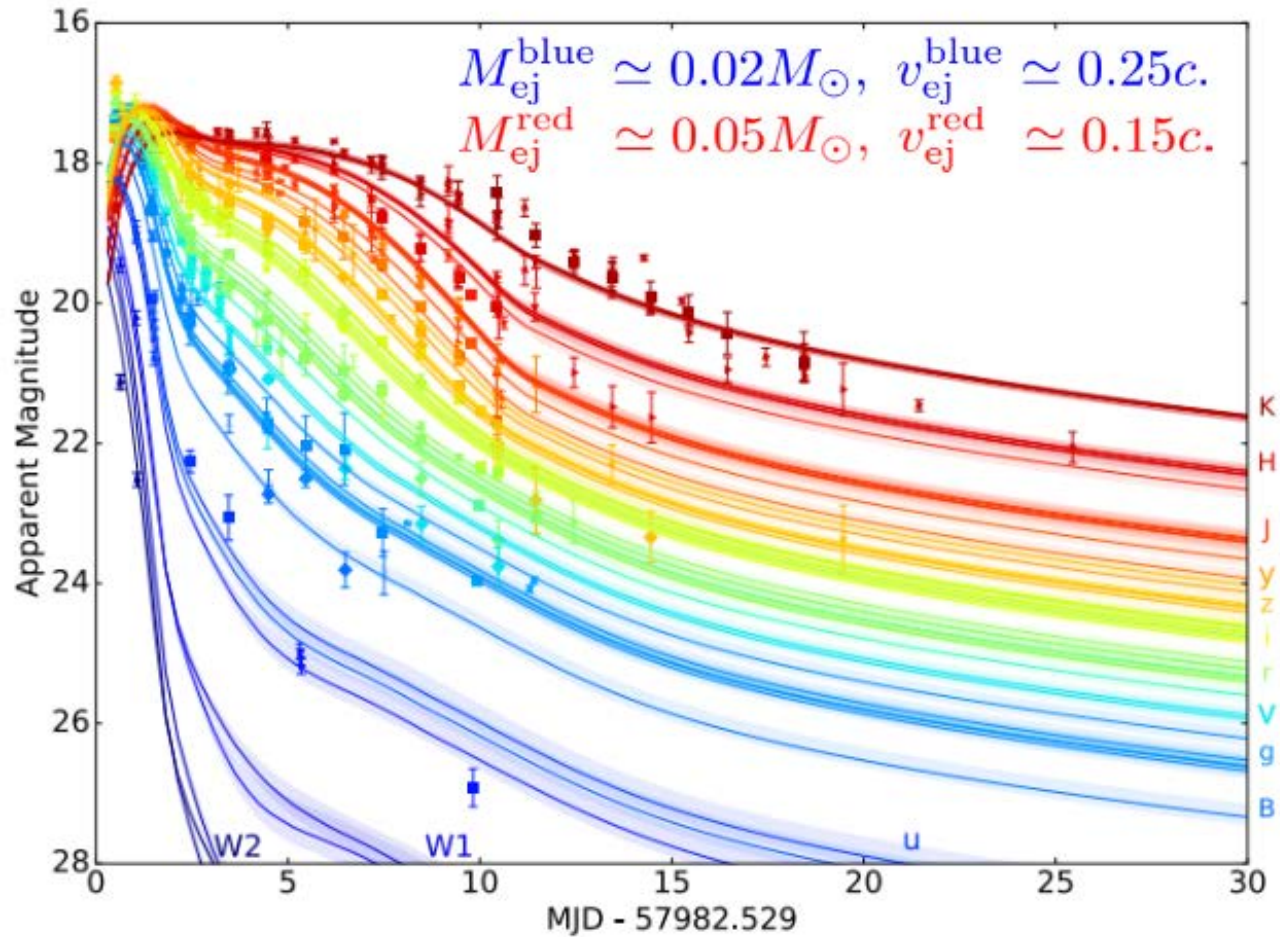


Figure. From Villar et al (2017)

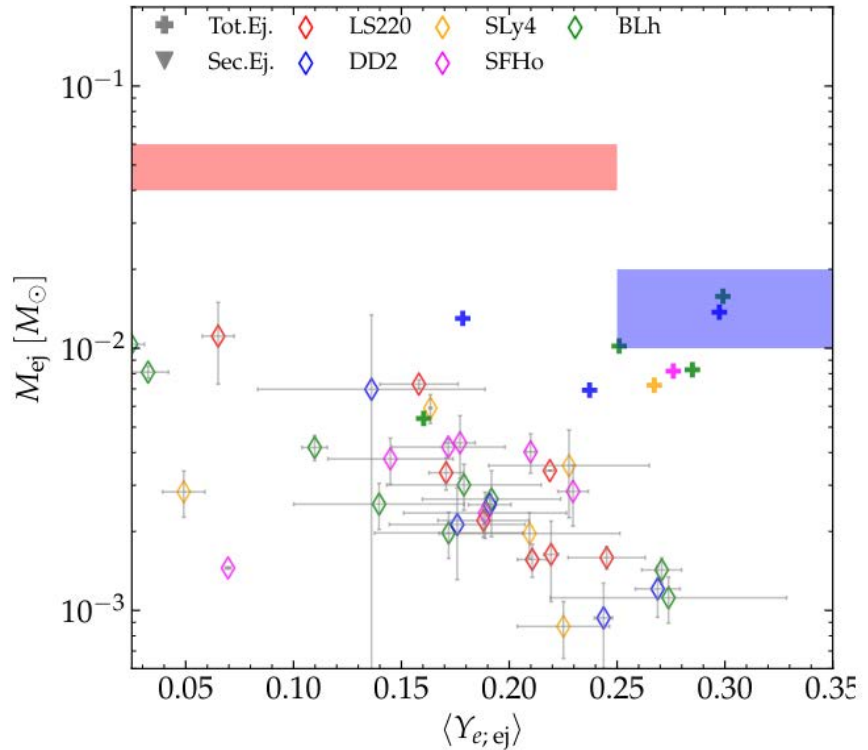
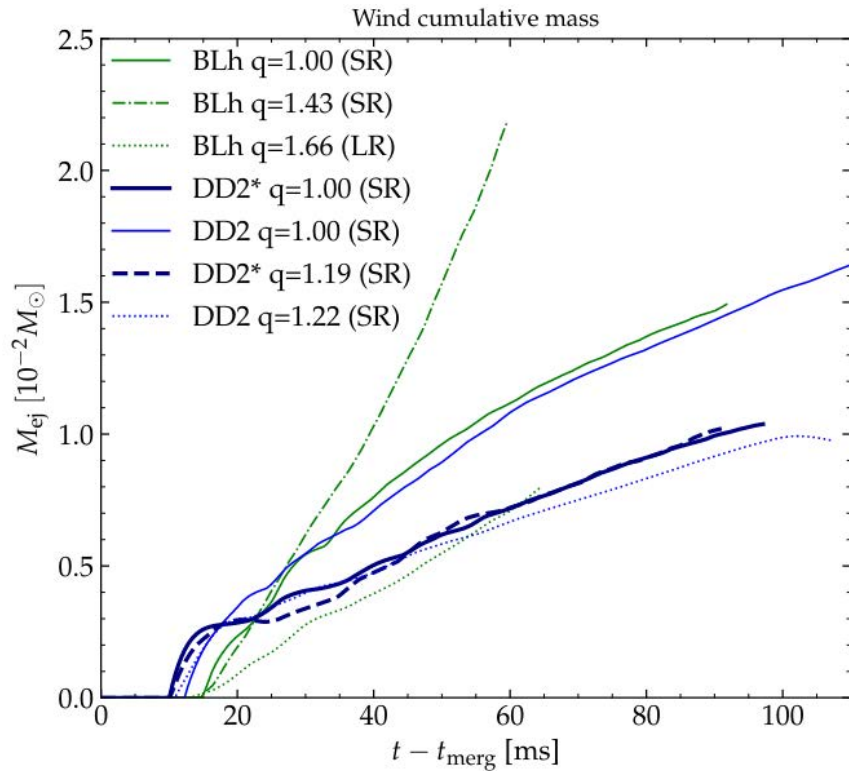
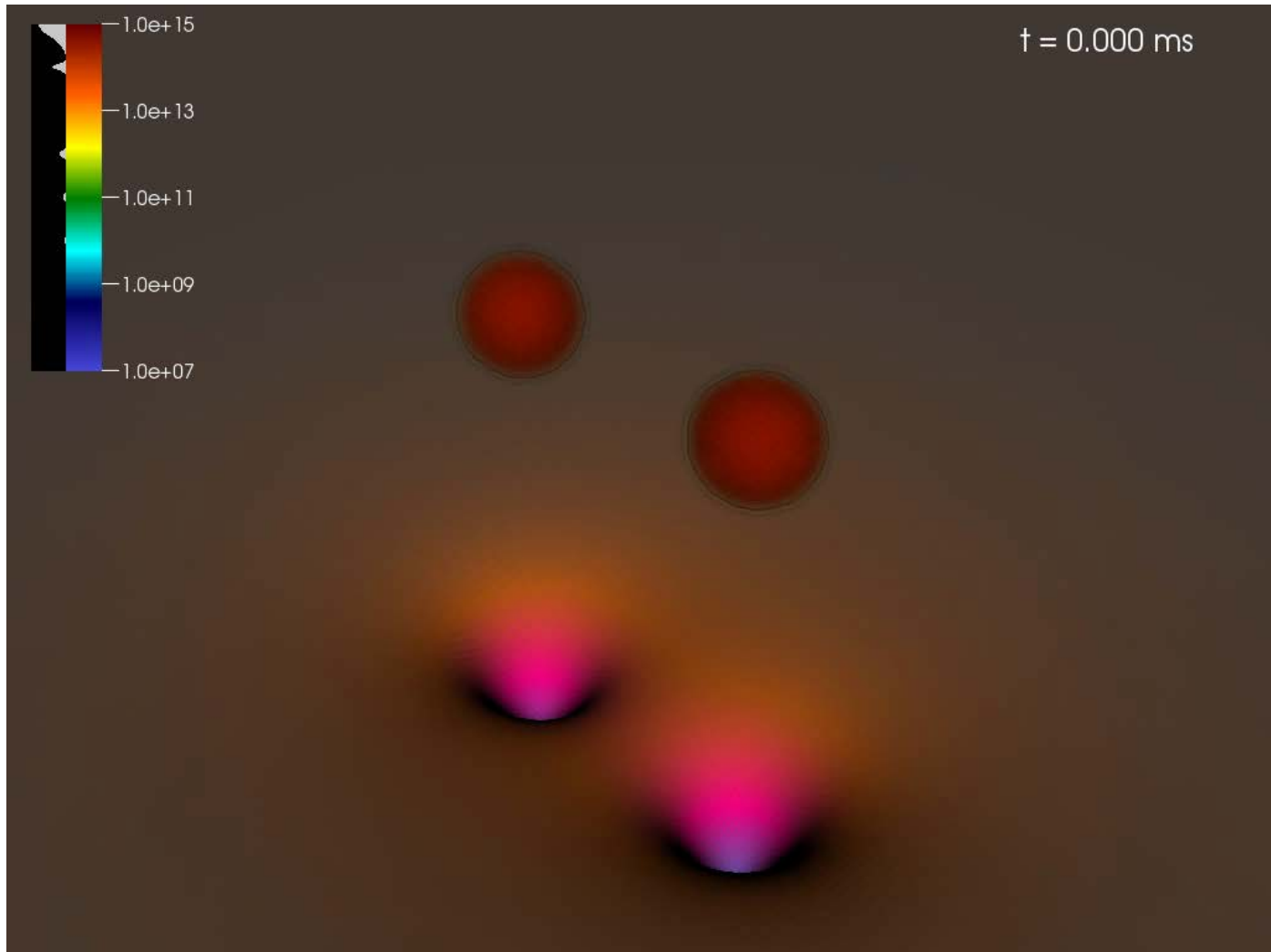


Figure. From Nedora et al. (2020)



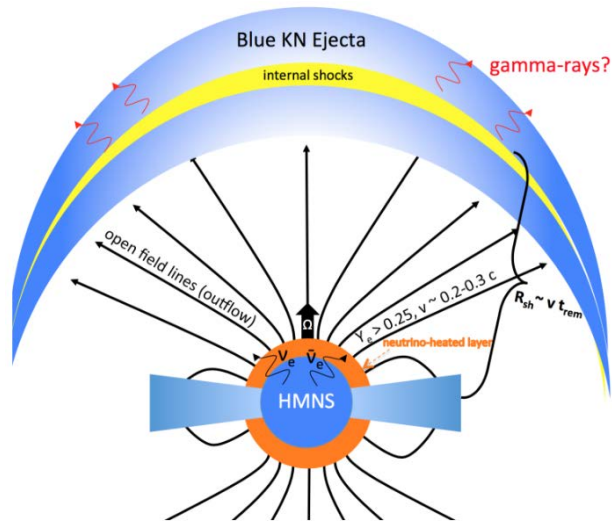


Figure. From Metzger et al. (2018)



Figure. From Mösta et al. (2020)

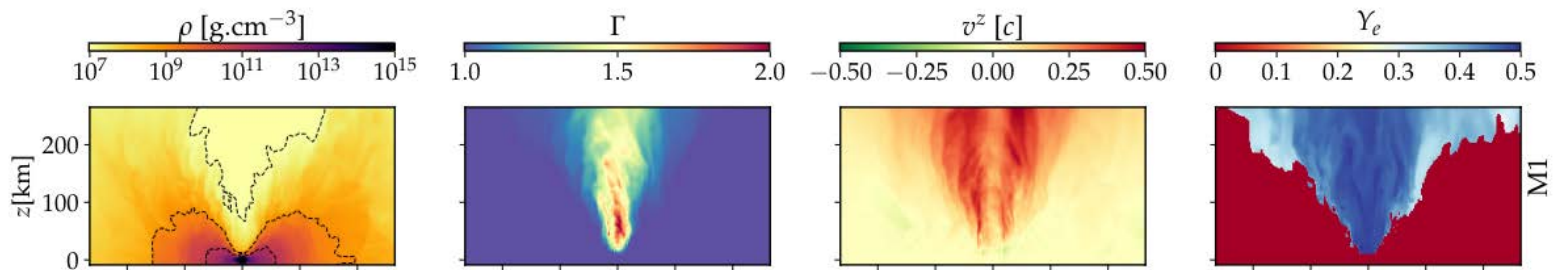


Figure. From Curtis et al. (2023)

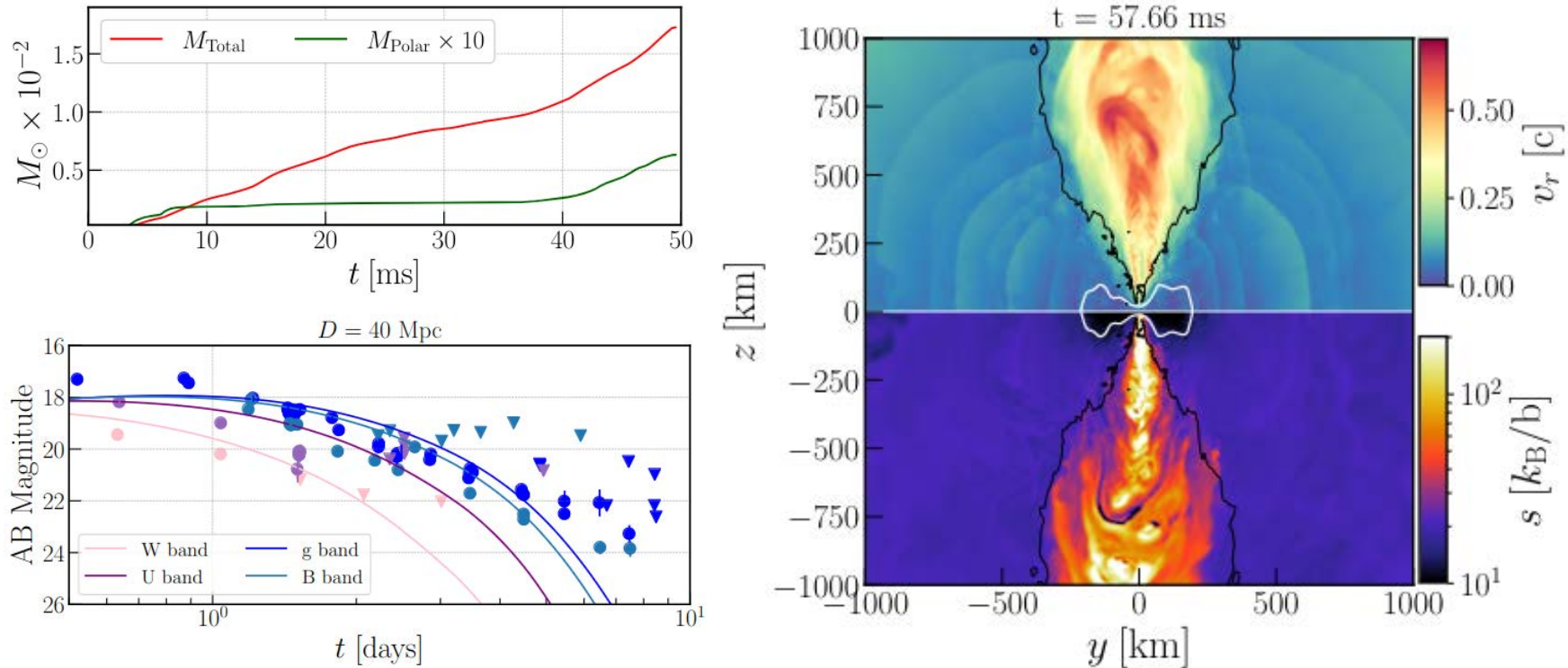


Figure. From Combi & Siegel (2023)

- Strong magnetic fields can suppress the low- $T/|W|$ instability
- What is the timescale for dynamo action in NS mergers?

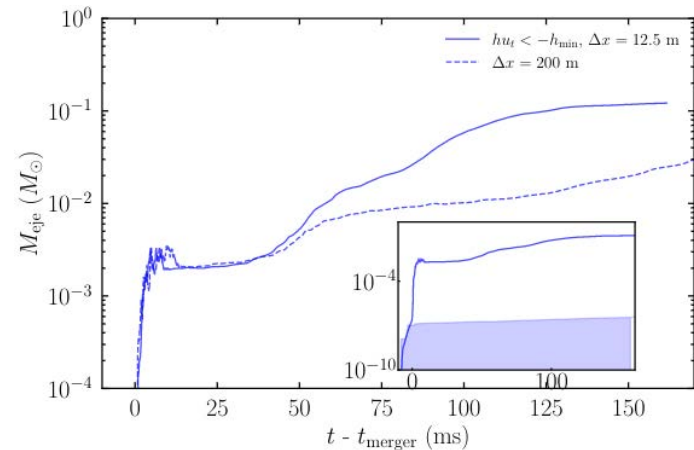
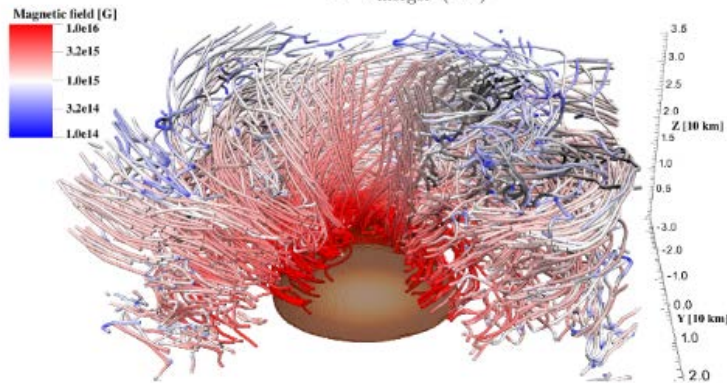
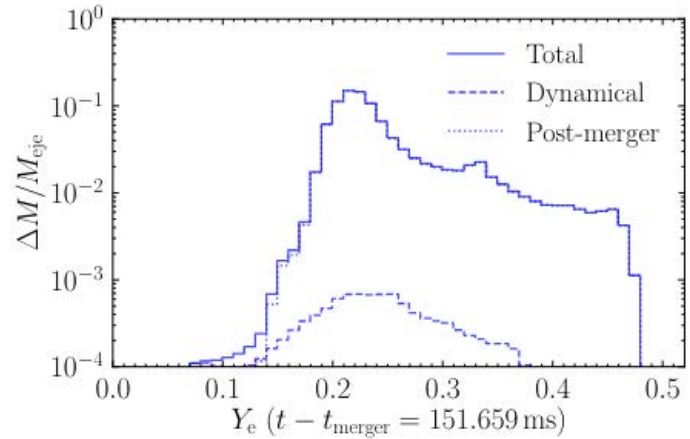
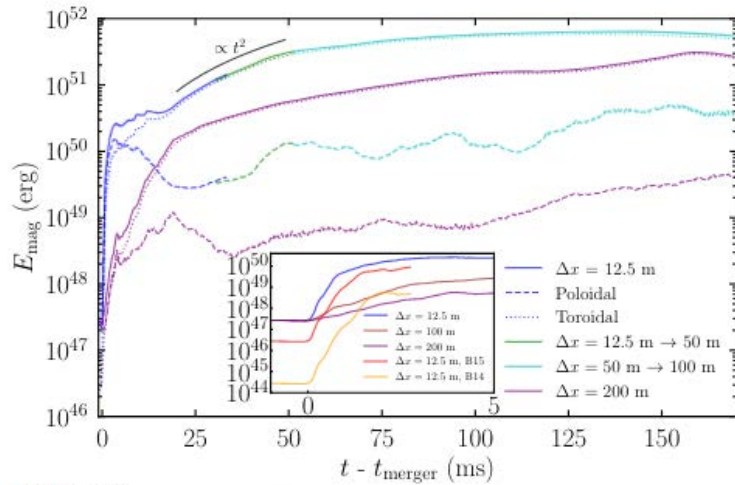


Figure. From Kiuchi et al. (2023)

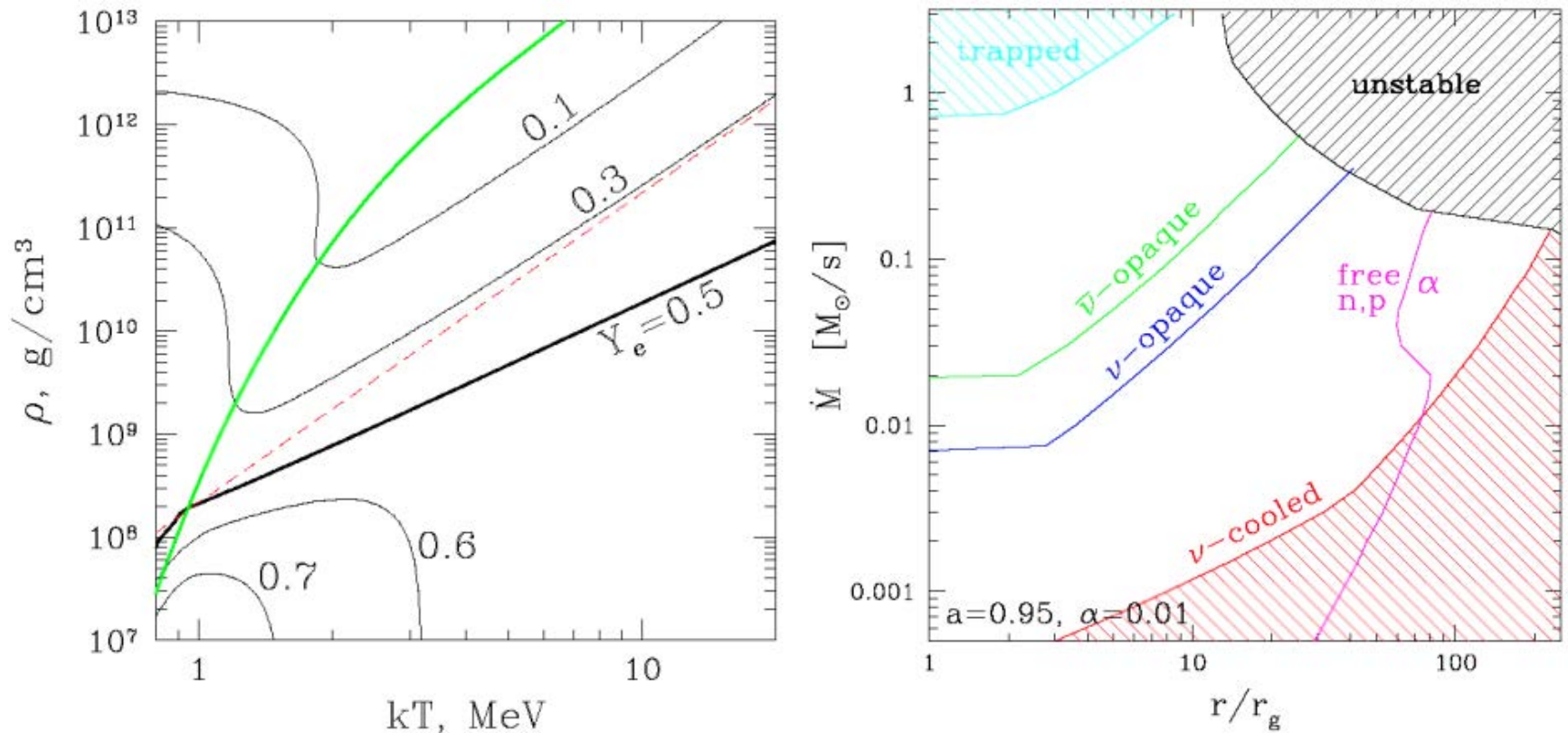


Figure. Equilibrium Y_e and phase diagram for neutrino-cooled accretion disks. From Beloborodov (2008).

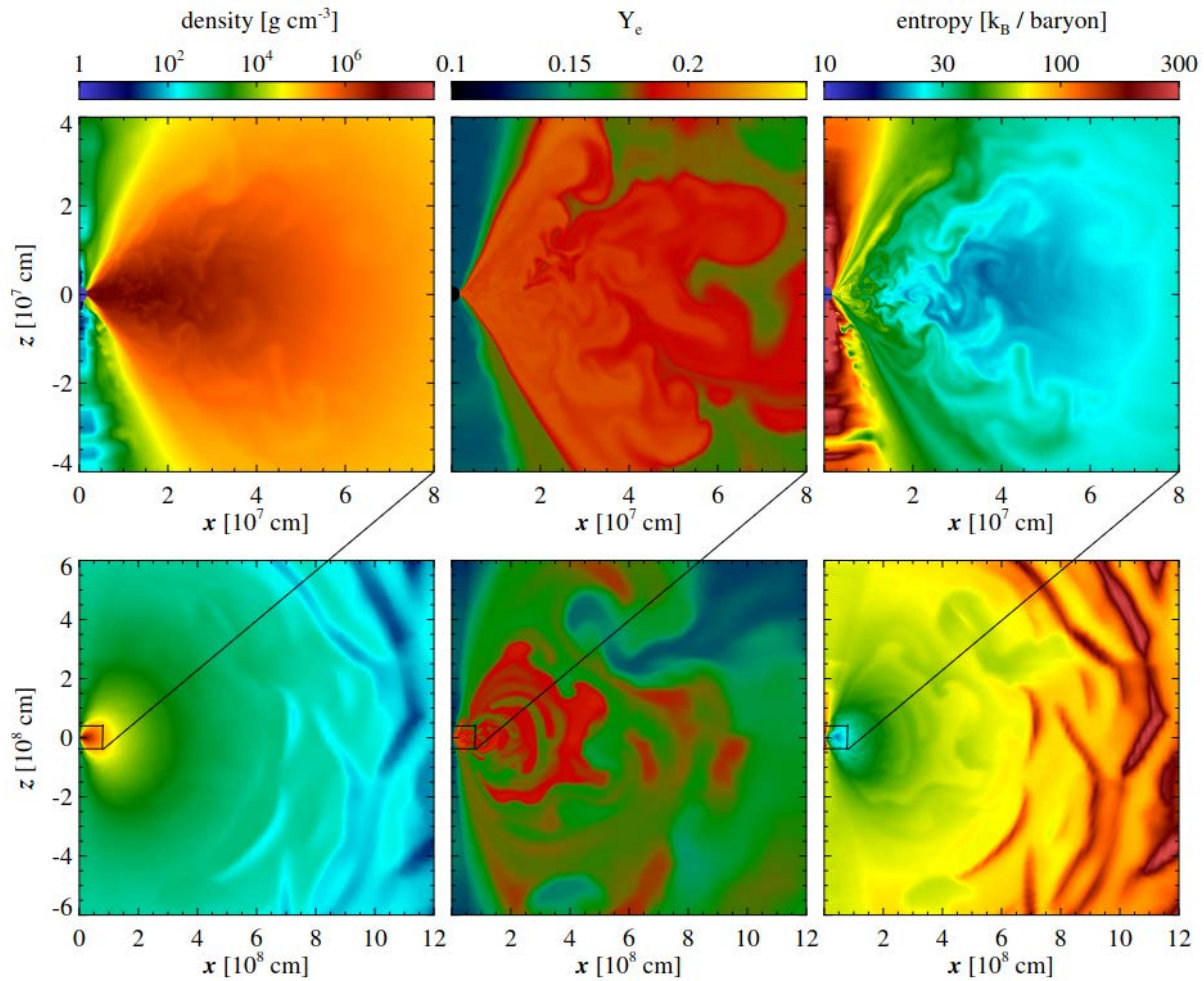


Figure. From Fernández and Metzger (2013)

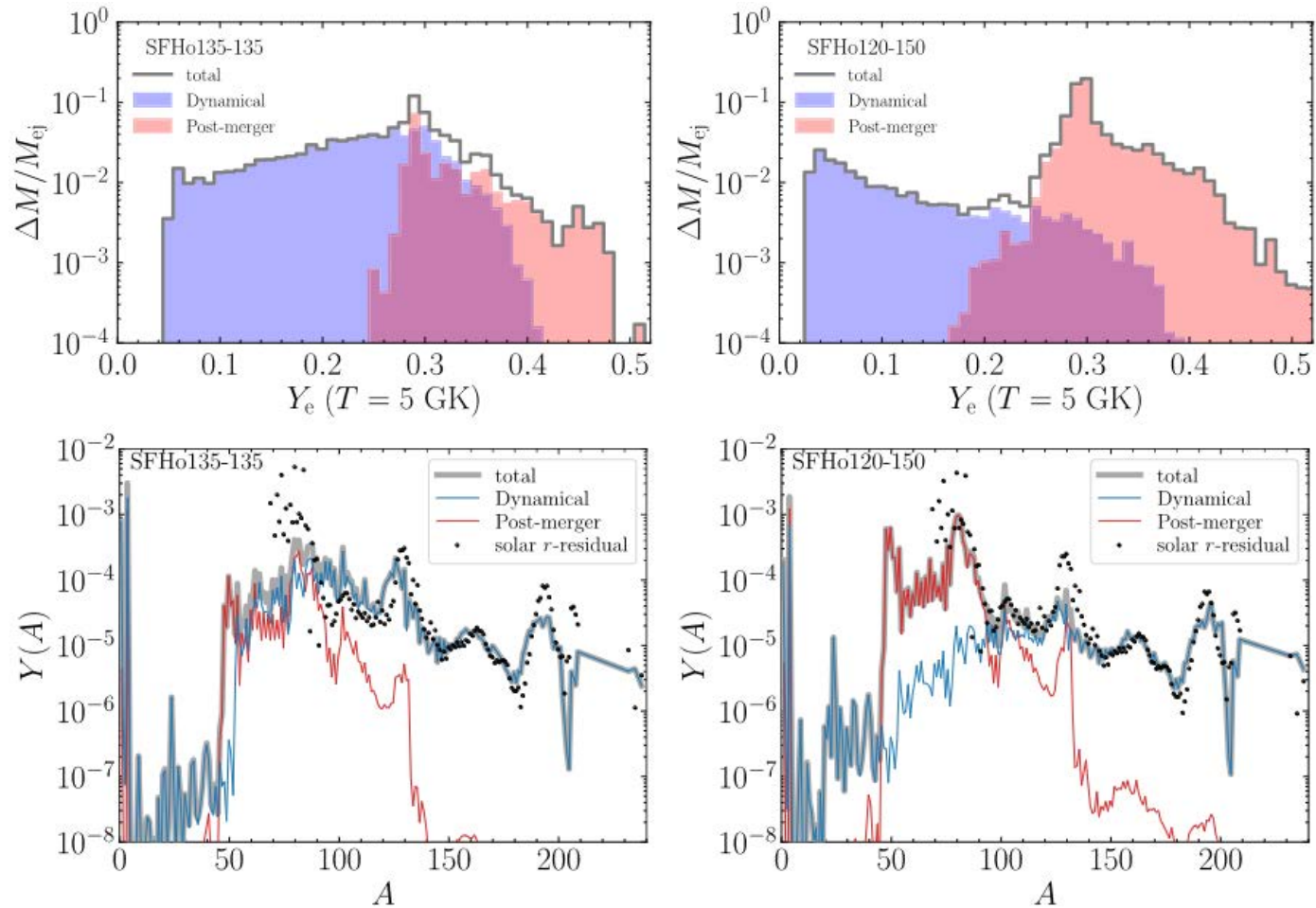


Figure. From Fujibayashi et al. (2023)

Fernández and Metzger showed that disk evaporation winds can be very neutron rich (**red kilonova**), unless irradiated by a massive neutron star remnant (**blue kilonova**):

When BH formation is relatively prompt (~ 100 ms), outflows from the disc are sufficiently neutron rich [...] In contrast, delayed BH formation allows neutrinos from the HMNS to raise the electron fraction in the polar direction.

Metzger and Fernandez (2014)

Fernández and Metzger showed that disk evaporation winds can be very neutron rich (**red kilonova**), unless irradiated by a massive neutron star remnant (**blue kilonova**):

When BH formation is relatively prompt (~ 100 ms), outflows from the disc are sufficiently neutron rich [...] In contrast, delayed BH formation allows neutrinos from the HMNS to raise the electron fraction in the polar direction.

Metzger and Fernandez (2014)

AT2017gfo had **both** a blue and a red kilonova.

- The expansion velocity and total mass of the blue kilonova made it challenging to explain with winds and the mass is too large for the shocked ejecta.
- The red kilonova has v_{ej} and Y_e consistent with disk winds (too slow for the dynamical ejecta), but M_{ej} implies a very massive disk, optically thick to neutrinos.

Fernández and Metzger showed that disk evaporation winds can be very neutron rich (**red kilonova**), unless irradiated by a massive neutron star remnant (**blue kilonova**):

When BH formation is relatively prompt (~ 100 ms), outflows from the disc are sufficiently neutron rich [...] In contrast, delayed BH formation allows neutrinos from the HMNS to raise the electron fraction in the polar direction.

Metzger and Fernandez (2014)

AT2017gfo had **both** a blue and a red kilonova.

- The expansion velocity and total mass of the blue kilonova made it challenging to explain with winds and the mass is too large for the shocked ejecta.
- The red kilonova has v_{ej} and Y_e consistent with disk winds (too slow for the dynamical ejecta), but M_{ej} implies a very massive disk, optically thick to neutrinos.

Several models are now available to explain the blue kilonova (spiral-wave wind, MHD).

Fernández and Metzger showed that disk evaporation winds can be very neutron rich (**red kilonova**), unless irradiated by a massive neutron star remnant (**blue kilonova**):

When BH formation is relatively prompt (~ 100 ms), outflows from the disc are sufficiently neutron rich [...] In contrast, delayed BH formation allows neutrinos from the HMNS to raise the electron fraction in the polar direction.

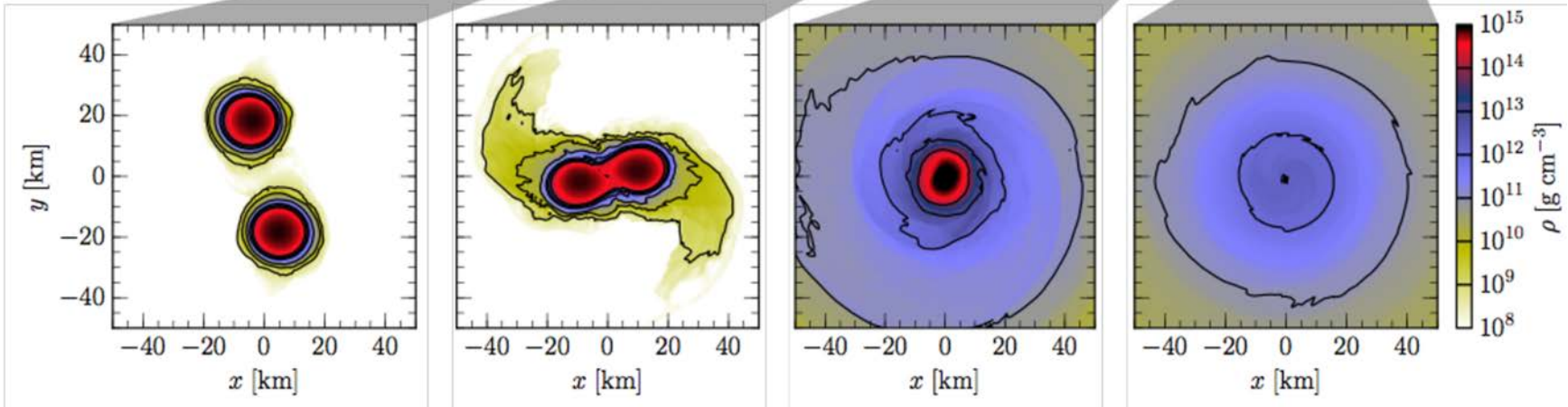
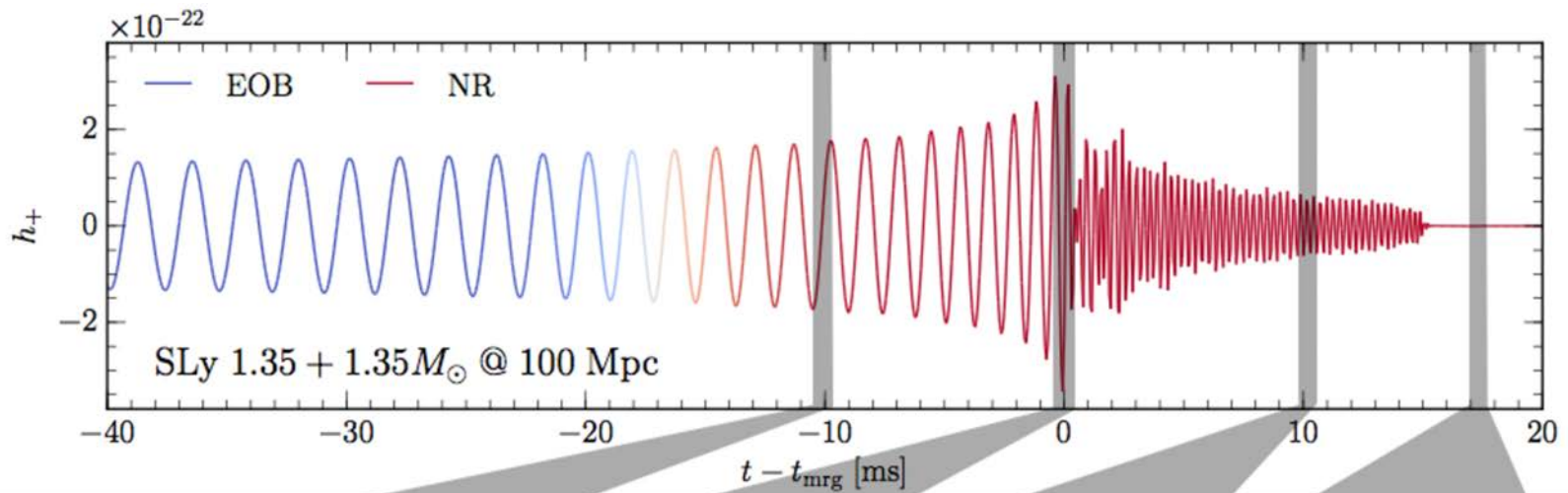
Metzger and Fernandez (2014)

AT2017gfo had **both** a blue and a red kilonova.

- The expansion velocity and total mass of the blue kilonova made it challenging to explain with winds and the mass is too large for the shocked ejecta.
- The red kilonova has v_{ej} and Y_e consistent with disk winds (too slow for the dynamical ejecta), but M_{ej} implies a very massive disk, optically thick to neutrinos.

Several models are now available to explain the blue kilonova (spiral-wave wind, MHD).

New simulations show that the Y_e of the disk wind ejecta is large, even for disks around BHs (Fujibayashi et al. 2023; Just et al. 2023). What is missing?



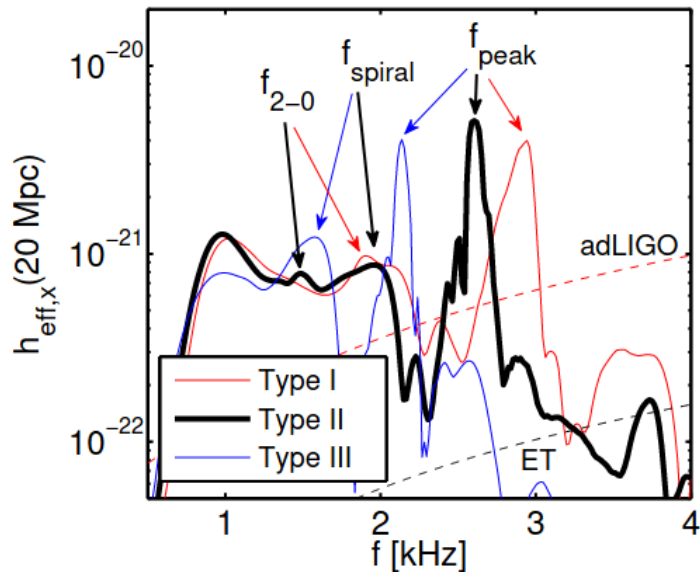


Figure. From Bauswein et al. (2015)

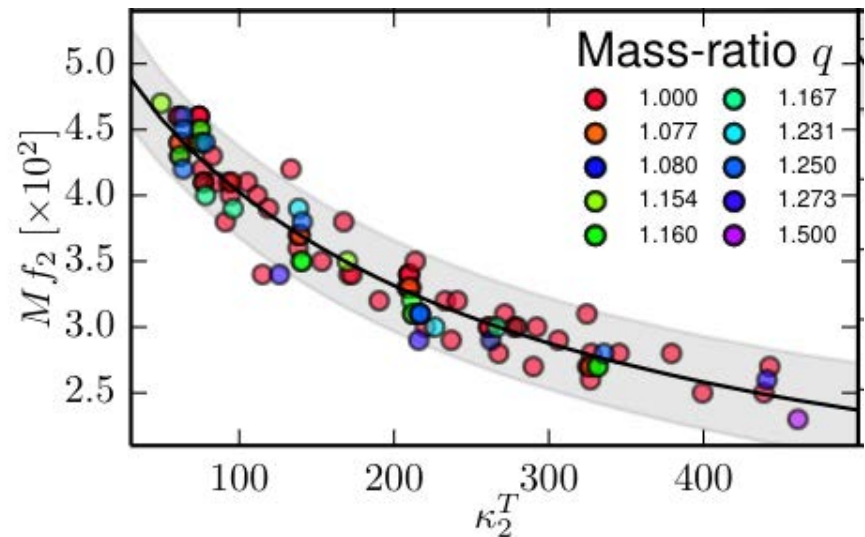


Figure. From Bernuzzi et al. (2015)

- The postmerger spectrum has characteristic frequencies that depend on the EOS
- The dominant frequency is f_{peak} or f_2 and is $2\Omega_{\text{rot}}$ of the remnant.
- Large literature, many ideas: Takami+ 2014; Bernuzzi 2015, Rezzolla+ 2016; Dietrich+ 2016; Breschi+ 2019; Bauswein+ 2019; Prakash+ 2021; Espino+ 2023 ...

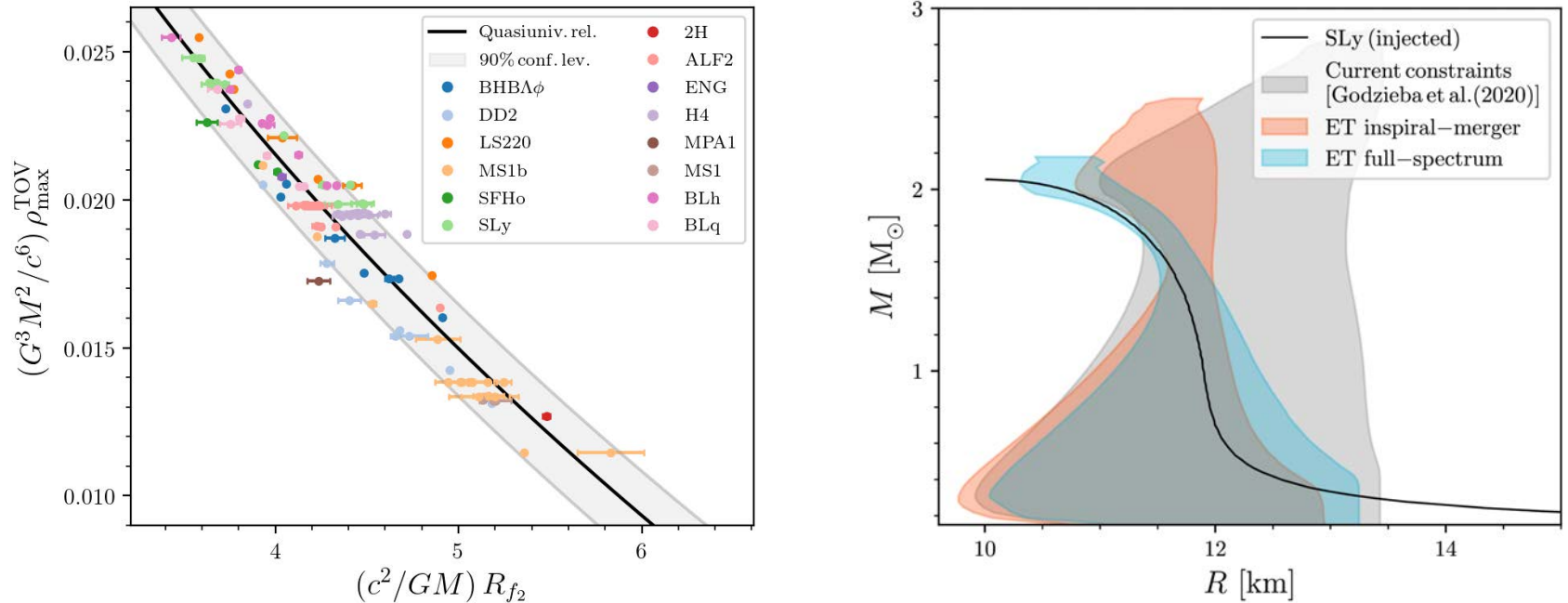


Figure. From Breschi et al. (2022)

- Binding energy of the remnant (Radice+ 2016)
- Phase transitions (Bauswein+ 2019; Prakash+ 2022; Espino+ 2023)
- Finite temperature effects (Fields+ 2023; Raithel+ 2023)

- Long-term evolution of massive neutron star remnants formed in mergers
- Gravitational waves modeling
 - Waveform models for next-generation detectors
 - Dynamical tides, excitation of modes in the stars
 - Post-merger signal: microphysics and MHD effects
- Mass ejection and nucleosynthesis
 - Self-consistent long-term evolution of NS mergers
 - Better neutrino transport
 - Neutrino oscillations
 - Self-consistent kilonova / merger models

- T. Baumgarte and S. Shapiro, *Numerical Relativity: Solving Einstein's Equations on the Computer*, Cambridge University Press (2010).
- A. M. Beloborodov, AIP Conf. Proc. **1054** (2008), 51 doi:10.1063/1.3002509.
- R. Fernández and B. D. Metzger, Ann. Rev. Nucl. Part. Sci. **66** (2016), 23-45 doi:10.1146/annurev-nucl-102115-044819.
- K. Kyutoku, M. Shibata and K. Taniguchi, Living Rev. Rel. **24** (2021) no.1, 5 doi:10.1007/s41114-021-00033-4.
- M. Shibata and K. Hotokezaka, Ann. Rev. Nucl. Part. Sci. **69** (2019), 41-64 doi:10.1146/annurev-nucl-101918-023625.
- D. Radice, S. Bernuzzi and A. Perego, Ann. Rev. Nucl. Part. Sci. **70** (2020), 95-119 doi:10.1146/annurev-nucl-013120-114541.